



MASTERARBEIT

Titel der Masterarbeit

Feasibility study for measurement of
general relativistic time dilations and gravitational phase shifts
on single photons

verfasst von

Tobias Schäfer, BSc

angestrebter akademischer Grad

Master of Science (MSc)

Wien, 2015

Studienkennzahl lt. Studienblatt:

A 066 876

Studienrichtung lt. Studienblatt:

Masterstudium Physik UG2002

Betreut von:

Univ.-Prof. Dr. Časlav Brukner

Abstract

It is known that gravity can bend or slow down classical light. But the influence of gravity on single photons has not been tested so far. Here the influence of gravity on single photons in quantum optical experiments is of interest. In particular such influence on single photons in a superposition of different regions of gravitational potential is considered. When only Newtonian gravity is assumed a gravitational scalar Aharonov-Bohm like phase occurs. Yet, treating gravity as locally equivalent to an accelerating reference frame, like in the general theory of relativity, the Shapiro delay could affect the coherence of the photon's superposition. A measurement of effects which are explainable only by such a gravitational time dilation can be viewed as the first experiment where both theories, quantum mechanics and general relativity, are essential to predict the outcome. Since, on earth, this effect is acutely small a direct measurement which was already suggested [1] is unpromising. In this thesis five methods which base on the amplification effect of postselections are analysed concerning their experimental feasibility in order to verify gravitational time dilations or gravitational phase shifts on single photons. Two of them directly base on the well-known weak measurement approach with postselections. It turns out that these methods could be used to reach a significant improvement in the experimental feasibility. While in [1] the required surface of the interferometer was calculated as 10^3 km^2 an improvement of five orders of magnitude is presented here. Moreover they can be used to detect any kind of time dilations or phase shifts which occur in interferometric experiments.

Zusammenfassung

Es ist bekannt, dass Gravitation klassisches Licht sowohl krümmen, als auch verlangsamen kann. Jedoch wurde die Wirkung von Gravitation auf einzelne Photonen bis heute noch nicht getestet. In dieser Arbeit steht der Einfluss von Gravitation auf einzelne Photonen in quantenoptischen Experimenten im Mittelpunkt. Im Speziellen wird der Einfluss von Gravitation auf Photonen in einer Superposition verschiedener Regionen des Gravitationspotentials betrachtet. Verwendet man die Newtonsche Gravitationstheorie könnte eine relative Phase, analog zur skalaren Aharonov-Bohm Phase, auftauchen. Behandelt man dagegen Gravitation als lokal äquivalent zu einem beschleunigten Bezugssystem, wie in der Allgemeinen Relativitätstheorie, könnte die Shapiro-Verzögerung die Kohärenz der Photonen beeinflussen. Eine Messung solcher Effekte, die allein durch gravitative Zeitdilatation erklärt werden können, wäre das erste Experiment, bei dem sowohl Quantenmechanik als auch Allgemeine Relativitätstheorie essentiell sind, um das Ergebnis vorherzusagen. Da der Effekt auf der Erde äußerst klein ist, ist eine direkte Messung, wie sie bereits in [1] vorgeschlagen wurde, äußerst unwahrscheinlich. Um gravitative Zeitdilatationen oder gravitative Phasenverschiebungen auf einzelnen Photonen den-

noch messen zu können, werden in dieser Arbeit fünf Methoden auf ihre Durchführbarkeit analysiert. Die Methoden basieren auf dem Verstärkungseffekt durch postselections. Zwei von ihnen beruhen direkt auf dem bekannten Verfahren der schwachen Messung mit postselections. Es stellt sich heraus, dass die Durchführbarkeit des Experiments durch diese Methoden signifikant verbessert werden kann. Während in [1] noch ein Interferometer, das eine Fläche von 10^3 km^2 einschließt, vorgeschlagen wurde, wird hier eine Verbesserung um fünf Größenordnungen präsentiert. Darüber hinaus können sie genutzt werden, um jede beliebige Art von Zeitdilatationen oder Phasenverschiebungen in Interferometerexperimenten zu detektieren.

Contents

1	Introduction	1
2	Fundamental concepts	3
2.1	Gravitational time dilation, redshift and the Shapiro delay	3
2.2	Quantum superposition, interference and which-path information	7
2.3	An interplay between QM interference and GR time dilation	10
3	Weak measurements	13
4	Optical interferometer: Setup and theoretical approach	17
4.1	Gravitational time dilation in a Mach-Zehnder interferometer	17
4.2	Newtonian Limit	20
4.3	Alternative setup: Michelson-Morley interferometer	21
5	Methods and results	25
5.1	Method 1: Amplified shifts of the mean frequency and mean arrival time . . .	27
5.2	Method 2: Phase amplification via postselections	31
5.3	Method 3: Additional controllable time delay	35
5.4	Method 4: Shaping double-humped photons	41
5.5	Method 5: Cutting out frequencies	53
6	Conclusion	59

1 Introduction

Although the research on quantum mechanics and quantum field theory on curved space-time looks back on decades, there is still a lack of experiments or proposals for feasible experiments which could probe an interplay between the fundamentals of quantum mechanics and general relativity. Since, from historical perspective, the progress in physics is predominantly driven by experiments, coming up with such experiments can provide an important contribution to the goal of a unified theory.

In 2011 Zych, Costa, Pikovski and Brukner published a thought experiment of this kind [2]. They propose a simple Mach-Zehnder setup placed in the gravitational field of the earth such that different amount of proper time elapses along each of the interferometer arms. Interference of single particles with internal time-evolving degrees of freedom serving as a clock is considered in this setup. Due to the gravitational time dilation the clock reveals which-path information. In combination with the complementarity principle, this can be understood as a gravitationally induced mechanism of losses and revival of coherence. Note that in this context the complementarity principle states the dichotomy between which-path information and the visibility of interference. Realising an experiment of this kind could be viewed as the first verification of general relativistic proper time in a quantum experiment.

A related paper was published later analysing the previously suggested experiment with the particular choice of single photons as particles [1]. In this case the distance taken by the photon is analogous to the mentioned internal degree of freedom serving as a clock. Even though optical interferometers are in general more feasible than interferometry with matter the major problem of this approach is the required size of the interferometer. For a significant drop of the visibility of the interference the gravitational time dilation must be of the order of the coherence time (pulse width) of the photon. According to the results of [1] the interferometer arms need to enclose an area of 10^3 km^2 , even if pulses with a coherence length of femtoseconds are used. Since such a size is far beyond what is feasible with current technology other approaches are needed to measure the effect of gravitational time dilation.

In this thesis five different theoretical approaches are considered in order to getting closer to a possible experimental verification of general relativistic effects on single photons.

The thesis is structured as follows: The basic concepts and physical effects (e.g. superposition principle, gravitational time dilation) are presented in chapter 2. In chapter 3 the formalism of weak measurements is introduced in order to apply it for the situation of a single photon travelling through a gravitationally influenced interferometer whose setup is presented in chapter 4. In section 5 five methods are suggested which base on amplification effects of postselections. Two of them directly use the weak measurement formalism. The five methods are: (1) Detecting amplified shifts in the mean frequency or in the mean arrival time of the photon, (2) Amplifying the gravitationally induced phase shift via postselection, (3) Improving the original visibility approach by using different pulse shapes or an additional controllable time delay, (4) Deforming the double-humped photon shape in dependence of the gravitational phase shift, and finally (5) Cutting out certain frequencies of the photons in dependence of the gravitational phase shift.

Two of these methods (1 and 3) directly probe the gravitational time dilation whereas three

(2, 4 and 5) are only consequences of the gravitational phase shift. However, a verification of the latter is not a proof of the existence of the former because a gravitational phase shift can also be explained via a gravitational scalar Aharonov-Bohm phase within Newtonian gravity if the photon couples to the gravitational potential. This phase occurs even if the force is the same on both paths. Although in such experiments the gravitational time dilation cannot be probed, the mass-energy equivalence for single photons can be tested.

2 Fundamental concepts

In this section the fundamental concepts crucial for this thesis are explained briefly to emphasise their meaning. Knowledge of the mathematical formalism of general relativity and quantum mechanics is assumed.

First gravitational time dilation is shown to be a consequence of the theory of general relativity. The gravitational redshift and the Shapiro delay are also derived as related effects. Second quantum mechanical superposition is introduced. The two papers [2] and [1], which build the fundament of this thesis, are presented, in order to demonstrate an interplay between quantum mechanics and gravity.

2.1 Gravitational time dilation, redshift and the Shapiro delay

Gravitational time dilation is a consequence of the different flow of time measured by a clock in different space-time regions. For example, a clock on the surface of the earth runs slower than a clock on a tower.

To derive this effect quantitatively within general relativity the Schwarzschild metric is assumed to be a good approximation of the geometry of space-time on a planet. In Schwarzschild coordinates (t, r, θ, φ) the Schwarzschild metric g can be written as

$$g = -c^2 \left(1 - \frac{2GM}{c^2 r} \right) dt^2 + \frac{1}{1 - \frac{2GM}{c^2 r}} dr^2 + r^2 d\theta^2 + r^2 \sin^2 \theta d\varphi^2, \quad (1)$$

where c is the speed of light, G is the gravitational constant and M is the mass of the planet. The signature $(-+++)$ is used for the metric. Two stationary observers with identical constant angular coordinates θ_0, φ_0 are located at R_1 (say on the earth's surface) and at $R_2 > R_1$ (say on a tower). Their world lines can be written as $x_i(\tau) = (t_i(\tau), R_i, \theta_0, \varphi_0)$, $i = 1, 2$, where the parameter τ is the proper time. The proper time is the elapsing time as measured by an ideal clock moving along the given world line. It is defined as the parameter of the world line such that the length $g\left(\frac{dx_i}{d\tau}, \frac{dx_i}{d\tau}\right)$ of the four-velocity $\frac{dx_i}{d\tau}$ is equal to $-c^2$. So the flow of the time coordinate $t_i(\tau)$ of the stationary observers can be found via

$$-c^2 = g\left(\frac{dx_i}{d\tau}, \frac{dx_i}{d\tau}\right) = \sum_{\alpha\beta} g_{\alpha\beta} \frac{dx_i^\alpha}{d\tau} \frac{dx_i^\beta}{d\tau} = -c^2 \left(1 - \frac{2GM}{c^2 R_i} \right) \left(\frac{dt_i}{d\tau} \right)^2, \quad (2)$$

leading to

$$t_i(\tau) = \frac{\tau}{\sqrt{1 - \frac{2GM}{c^2 R_i}}}. \quad (3)$$

This equation shows that in order to pass the same amount of coordinate time, the elapsed proper time (the time of the clock of a stationary observer) is different for the two observers. Consider, e.g., two spatial fixed events with time coordinates separated by Δt . According to (3) observer 1 measures a proper time interval of

$$\Delta\tau_1 = \sqrt{1 - \frac{2GM}{c^2 R_1}} \Delta t \quad (4)$$

with his clock, whereas observer 2 measures

$$\Delta\tau_2 = \sqrt{1 - \frac{2GM}{c^2 R_2}} \Delta t . \quad (5)$$

A suitable form to express this time dilation is the ration between $\Delta\tau_2$ and $\Delta\tau_1$:

$$\frac{\Delta\tau_2}{\Delta\tau_1} = \frac{\sqrt{1 - \frac{2GM}{c^2 R_2}}}{\sqrt{1 - \frac{2GM}{c^2 R_1}}} . \quad (6)$$

The ratio (6) can be expressed as a function of the measurable proper distance h of the two stationary observers. The proper distance h is the distance between the two stationary observers as measured by a ruler. It is defined by the length of the space-like curve $\gamma(\lambda) = (t_0, R_1 + \lambda(R_2 - R_1), \theta_0, \varphi_0)$ extending from R_1 (at $\lambda = 0$) to R_2 (at $\lambda = 1$) where the coordinate time t_0 is constant:

$$h = \int_0^1 \sqrt{g \left(\frac{d\gamma}{d\lambda}, \frac{d\gamma}{d\lambda} \right)} d\lambda = \int_{R_1}^{R_2} \frac{1}{\sqrt{1 - \frac{2GM}{c^2 r}}} dr . \quad (7)$$

Note that for $M \neq 0$ the proper distance h is different to the coordinate distance $R_2 - R_1$. In general the proper distance between two space-like separated events ($dt = 0$) is an invariant length measure in general relativity. Assuming $\frac{\Delta R}{R_1} := \frac{R_2 - R_1}{R_1}$ to be very small (i.e. the two observers are close to each other as compared to the radius of the earth) the time dilation can be approximated as

$$\frac{\Delta\tau_2}{\Delta\tau_1} = \frac{\sqrt{1 - \frac{2GM}{c^2 R_1(1 + \Delta R/R_1)}}}{\sqrt{1 - \frac{2GM}{c^2 R_1}}} = 1 + \frac{1}{1 - \frac{2GM}{c^2 R_1}} \frac{GM}{c^2 R_1} \frac{\Delta R}{R_1} + \mathcal{O} \left(\frac{\Delta R}{R_1} \right)^2 . \quad (8)$$

Furthermore h can be approximated as

$$h = \frac{R_1}{\sqrt{1 - \frac{2GM}{c^2 R_1}}} \frac{\Delta R}{R_1} + \mathcal{O} \left(\frac{\Delta R}{R_1} \right)^2 , \quad (9)$$

leading to

$$\frac{\Delta\tau_2}{\Delta\tau_1} \approx 1 + \frac{gh}{c^2} \frac{1}{\sqrt{1 - \frac{2GM}{c^2 R_1}}} , \quad (10)$$

where g is the gravitational acceleration on earth. Furthermore, on earth, the square root can, in the last step, be approximated as 1 to obtain

$$\frac{\Delta\tau_2}{\Delta\tau_1} \approx 1 + \frac{gh}{c^2} . \quad (11)$$

The first experimental test of gravitational time dilation was the Hafele-Keating experiment in 1971 [3], [4]. Four previously synchronised atomic clocks were compared after several hours, where two of them stayed on the ground and two of them flew in an airplane at an altitude of 10 km. Note that in this experiment the measured time dilation was originated not only by the gravitational time dilation but also by kinematic effects like special relativistic time dilation and the Sagnac effect.

Gravitational redshift

Light leaving a source with a certain frequency will be measured to have a different frequency in different space-time regions. For example, sending light from the surface of the earth to the top of a tower decreases the frequency of the light (redshift).

The effect of the gravitational redshift is related to the gravitational time dilation. This is due to the fact that the frequency of light is nothing but the inverse of the period of the propagating light wave. Since time dilation also affects this period, gravitational redshift is a consequence of gravitational time dilation.

For a simple mathematical derivation consider two radial null geodesics in the Schwarzschild metric (1) representing two sequent wave crests of a light wave. A curve $\gamma(\tau)$ in space-time is called to be null or light-like if $g\left(\frac{d\gamma}{d\tau}, \frac{d\gamma}{d\tau}\right) = 0$ where τ is the proper time. It is called radial if the angular coordinates are constant. The geodesics of the wave crests pass a fixed point in space (say the light source on earth's surface) at R_1 at different coordinate times separated by Δt . For null geodesics one gets from (1) the relation

$$cdt = \frac{1}{1 - \frac{2GM}{c^2 r}} dr \quad (12)$$

between r and t . Since the right hand side is independent of t both crests pass the observer at $R_2 > R_1$ (say on a tower) with the same difference in coordinate time Δt . According to (4) and (5) an observer at the earth's surface will measure a different period $\Delta\tau_1$ of the wave than an observer on the tower $\Delta\tau_2$. Since frequency is nothing but the inverse of the period $\nu_i = 1/\Delta\tau_i$ one obtains

$$\frac{\nu_1}{\nu_2} = \frac{\Delta\tau_2}{\Delta\tau_1} = \frac{\sqrt{1 - \frac{2GM}{c^2 R_2}}}{\sqrt{1 - \frac{2GM}{c^2 R_1}}}, \quad (13)$$

where ν_1 and ν_2 are the frequencies as measured on earth or on top of the tower respectively. Using the same approximation as in the previous section this formula can be expressed in terms of the height difference h of the observers:

$$\frac{\nu_1}{\nu_2} \approx 1 + \frac{gh}{c^2}. \quad (14)$$

Robert Pound and Glen A. Rebka were the first¹ who observed this redshift effect in the famous Pound-Rebka experiment in 1960 [6]. Gamma rays were sent 22.5 m from the bottom to the top of a tower. The Mössbauer effect was used to make sure that emitter and absorber have the same resonance frequency. According to the redshift the emitted gamma rays were only absorbed when the absorbers resonance frequency was modified by a Doppler shift due to additional relative motion.

The Shapiro delay

The speed of light, as measured by a stationary observer, is slowed down near massive objects which originate a gravitational potential. Again, this is an effect related to the gravitational time dilation. For a light-like curve the Shapiro delay can be defined as the difference between the elapsed coordinate time of a certain path in Minkowski space-time and the elapsed coordinate time of the same path in a curved space-time.

Consider a light-like radial geodesic in Minkowski space-time. The Minkowski metric in spherical coordinates is given by

$$\eta = -c^2 dt^2 + dr^2 + r^2 d\theta^2 + r^2 \sin^2 \theta d\varphi^2. \quad (15)$$

The elapsed coordinate time for light to travel from R_1 to $R_2 > R_1$ then is

$$\Delta t_M = \frac{R_2 - R_1}{c}. \quad (16)$$

In the Schwarzschild metric (1), in contrast, one gets for the elapsed coordinate time

$$\Delta t_S = \frac{1}{c} \int_{R_1}^{R_2} \frac{1}{1 - \frac{2GM}{c^2 r}} dr = \frac{R_2 - R_1}{c} + \frac{2GM}{c^3} \ln \left(\frac{R_2 - 2GM/c^2}{R_1 - 2GM/c^2} \right). \quad (17)$$

This can be used to define the Shapiro delay Δs as the difference between Δt_S and Δt_M :

$$\Delta s = \Delta t_S - \Delta t_M = \frac{2GM}{c^3} \ln \left(\frac{R_2 - 2GM/c^2}{R_1 - 2GM/c^2} \right). \quad (18)$$

Obviously $\Delta s > 0$ holds for all $R_2 > R_1 > 2GM/c^2$, hence more coordinate time and therefore more proper time (for any observer) passes in the presence of a massive object.

Its first observation was in 1966 and 1967 by Irwin Shapiro et al. [7]. They measured the time of a radar signal sent from earth and bounced off Venus in dependence of the position of the sun which served as the massive object.

¹Although Schiffer et al. [5] measured the gravitational red shift effect a few months before Pound and Rebka, the latter claimed that Schiffer et al. underrated the error which is originated by a temperature difference of the photon emitter and absorber.

2.2 Quantum superposition, interference and which-path information

The notion of a superposition of states is a foundational tenet of quantum mechanics. In textbooks it is usually introduced as the possibility to decompose a state into different bases where the factors in front of the basis vectors are interpreted as the probability amplitudes. Here, however, the difference between the *and* of a superposition and the *or* of a classical mixture is emphasised.

For the calculations the state operator formalism is used. A state is given by a linear, hermitian operator $\rho \in \mathcal{L}(\mathcal{H})$ on a Hilbert space \mathcal{H} satisfying

$$\rho \geq 0, \quad \text{tr} \rho = 1. \quad (19)$$

A state is called pure if and only if $\text{tr} \rho^2 = 1$ or mixed if and only if $\text{tr} \rho^2 < 1$.

Consider now a setup where the space is divided into "above" and "below" a beam splitter (Fig. 1). The corresponding states are denoted as $|0\rangle$ and $|1\rangle$ respectively. Two states for a single particle will be considered. The first state ρ_1 is a classical balanced mixture of "above" and "below":

$$\rho_1 := \frac{1}{2}|0\rangle\langle 0| + \frac{1}{2}|1\rangle\langle 1|, \quad (20)$$

whereas the second state ρ_2 is a coherent balanced superposition of "above" and "below",

$$|S\rangle = \frac{1}{\sqrt{2}}(|0\rangle + |1\rangle), \quad (21)$$

leading to

$$\rho_2 := |S\rangle\langle S| = \frac{1}{2}|0\rangle\langle 0| + \frac{1}{2}|1\rangle\langle 1| + \frac{1}{2}|0\rangle\langle 1| + \frac{1}{2}|1\rangle\langle 0|. \quad (22)$$

The two detectors are represented by the measurement operators $D_0 = |0\rangle\langle 0|$ and $D_1 = |1\rangle\langle 1|$. Placing the detectors in front of the beam splitter (before the particle can reach the latter) the probabilities p_0 and p_1 to measure "above" or "below" are the same for both states:

$$p_0 = \text{tr} \rho_1 D_0 = \text{tr} \rho_2 D_0 = \frac{1}{2}, \quad p_1 = \text{tr} \rho_1 D_1 = \text{tr} \rho_2 D_1 = \frac{1}{2}. \quad (23)$$

Hence it is impossible to distinguish the states ρ_1 and ρ_2 in this setup. Putting the detectors back behind the beam splitter (like in Fig. 1) leads to interference effects which clearly shows the difference between a classical mixture ("either above *or* below") and a superposition (which is sometimes described as "both above *and* below at once"). Note that only one single particle is considered. The unitary transformation representing the balanced beam splitter is here given by

$$U_{\text{BS}} = \frac{1}{\sqrt{2}}(|0\rangle\langle 0| + |1\rangle\langle 0| + |0\rangle\langle 1| - |1\rangle\langle 1|). \quad (24)$$

The representation of the beam splitter can be constructed under the assumption that it creates coherent superpositions from pure states. If one starts with $U_{\text{BS}}|0\rangle := (|0\rangle + |1\rangle)/\sqrt{2}$, only one free parameter remains in order to keep the unitarity. This parameter turns out to

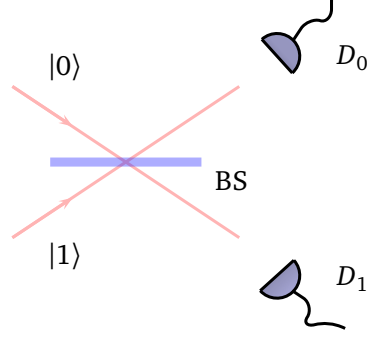


Figure 1: A simple setup with a beam splitter and two detectors to demonstrate the interference of a single particle in an initially superposed state.

be a relative phase (see below for the notion of a relative phase) and was arbitrarily chosen such that U_{BS} is pure real. So the states behind the beam splitter are

$$\rho_1 \xrightarrow{\text{BS}} \rho'_1 = U_{\text{BS}} \rho_1 U_{\text{BS}}^\dagger = \rho_1, \quad \rho_2 \xrightarrow{\text{BS}} \rho'_2 = U_{\text{BS}} \rho_2 U_{\text{BS}}^\dagger = |0\rangle\langle 0|. \quad (25)$$

Due to interference at the beam splitter the states ρ'_1 and ρ'_2 lead to different detection probabilities. For ρ'_1 one still gets

$$p_0 = \text{tr} \rho'_1 D_0 = \frac{1}{2}, \quad p_1 = \text{tr} \rho'_1 D_1 = \frac{1}{2}, \quad (26)$$

but ρ'_2 results in

$$p_0 = \text{tr} \rho'_2 D_0 = 1, \quad p_1 = \text{tr} \rho'_2 D_1 = 0. \quad (27)$$

A further difference between a classical mixture and a superposition is the relative phase, which, for a clear analogy to the mixed state, was chosen as 1 in (21). In the state operator representation the relative phases appear in the off-diagonal terms. How they affect the interference at a beam splitter is demonstrated in a Mach-Zehnder interferometer (Fig. 2): Let the incident particle be a pure state coming from below:

$$\rho = |1\rangle\langle 1|. \quad (28)$$

The whole interferometer then acts like a unitary

$$U_{\text{MZ}} = U_{\text{BS}} U_{\text{PS}} U_{\text{BS}}, \quad (29)$$

where U_{BS} is the action of the beam splitter (24) and

$$U_{\text{PS}} = e^{i\varphi} |0\rangle\langle 0| + |1\rangle\langle 1| \quad (30)$$

represents the phase shift which assigns a relative phase of $e^{i\varphi}$ to the upper path. The outgoing state ρ' is the unitary transformed incident state

$$\rho \xrightarrow{\text{MZ}} \rho' = U_{\text{MZ}} \rho U_{\text{MZ}}^\dagger = \sin^2 \frac{\varphi}{2} |0\rangle\langle 0| + \frac{i \sin \varphi}{2} |0\rangle\langle 1| - \frac{i \sin \varphi}{2} |1\rangle\langle 0| + \cos^2 \frac{\varphi}{2} |1\rangle\langle 1|. \quad (31)$$

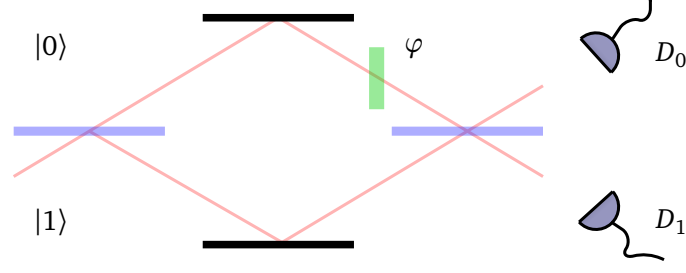


Figure 2: A Mach-Zehnder interferometer consisting of two beam splitters (blue), two mirrors (black), a phase shift element, and two detectors.

Hence the detection probabilities oscillate with the phase φ :

$$p_0 = \text{tr} \rho' D_0 = \sin^2 \frac{\varphi}{2}, \quad p_1 = \text{tr} \rho' D_1 = \cos^2 \frac{\varphi}{2}. \quad (32)$$

The visibility of the interference is defined via

$$\mathcal{V} = \frac{\max_{\varphi} [p_i] - \min_{\varphi} [p_i]}{\max_{\varphi} [p_i] + \min_{\varphi} [p_i]}, \quad i = 0, 1. \quad (33)$$

In the described Mach-Zehnder setup one clearly has $\mathcal{V} = 1$. The complementary quantity is the distinguishability \mathcal{D} , which is defined as the distance between the final detector states in the trace norm [8]. It represents the amount of which-path information and can be interpreted as the probability to correctly guess which path the particle took in the interferometer. Since due to the superposition one cannot guess better than randomly which path the particle took, the distinguishability is zero in the above example. The inequality $\mathcal{V}^2 + \mathcal{D}^2 \leq 1$ states the often-quoted complementarity principle. Note that the equality holds only for pure states (see [8] for a comprehensive derivation).

If, for some reason, it is possible to increase the probability to correctly guess which path the particle took (increase \mathcal{D}) this is at the expense of the visibility \mathcal{V} . In chapter 2.3 it will be shown under what conditions the gravitational time dilation can induce an increase of \mathcal{D} .

The first experimental test of the relation between the visibility \mathcal{V} and the distinguishability \mathcal{D} was done by Greenberger and Yasin in 1988 [9]. They used a neutron interferometer where one arm was equipped with an element blocking a certain percentage of the neutron beam to increase the distinguishability \mathcal{D} .

2.3 An interplay between QM interference and GR time dilation

In 2011 Zych, Costa, Pikovski and Brukner [2] published the idea of an

”interference of a clock”

which occurs in a Mach-Zehnder interferometer placed in the gravitational field if the used particle has some internal degree of freedom that evolves in time. This internal degree of freedom then serves as a clock measuring the proper time along its path. As the arms of the interferometer route through different space-time regions the flow of time is different along each arm. This affects the evolution of the clock states which become entangled with the path degree of freedom. As a result, the initially coherent superposition of the two paths becomes incoherent: The more distinguishable become the time dilated clock states, the more the total state is entangled and the less coherent becomes the path degree of freedom. The time dilation reveals which-path information and therefore increases the distinguishability and decreases the visibility of the interference. In difference to any other performed or proposed experiments where quantum mechanics and gravity interplay, the general relativistic notion of proper time is indispensable.

In order to review this idea shortly the next several equations are cited, with permission, from Zych et al. [2],[1]. A similar setup on which this thesis is based, is discussed in detail in ch. 4.

Inside the interferometer (see Fig. 3, reproduced with permission from Zych et al. [1]), just in front of the second beam splitter, the state of the particle reads :

$$|\psi\rangle = \frac{1}{\sqrt{2}}(ie^{-i\Phi_1}|r_1\rangle|\tau_1\rangle + e^{-i\Phi_2+i\varphi}|r_2\rangle|\tau_2\rangle) . \quad (\text{eq. (3) in [2]})$$

Here $|r_1\rangle$ and $|r_2\rangle$ are the path states (according to path γ_1 and γ_2 respectively) whereas $|\tau_1\rangle$ and $|\tau_2\rangle$ are the states of the internal degree of freedom acting as the clock. The trajectory dependent phases are denoted as Φ_1 and Φ_2 and φ is some additional controllable phase. The above state describes an entangled state, so in order to calculate the detection probabilities for the detectors D_{\pm} the internal degree of freedom has to be traced out after the second beam splitter. Hence the detection probabilities are

$$P_{\pm} = \frac{1}{2} \pm \frac{1}{2}|\langle\tau_1|\tau_2\rangle|\cos(\Delta\Phi + \alpha + \varphi) , \quad (\text{eq. (4) in [2]})$$

where $\Delta\Phi = \Phi_1 - \Phi_2$ and α is the phase of the complex number $\langle\tau_1|\tau_2\rangle$. According to the definition (33) the visibility reads

$$\mathcal{V} = |\langle\tau_1|\tau_2\rangle| . \quad (\text{eq. (5) in [2]})$$

Thus which-path information becomes available in dependence on the accuracy of the internal clock: The smaller $|\langle\tau_1|\tau_2\rangle| \leq 1$ for a fixed time dilation the higher the accuracy of the clock. In the case of a periodic clock one should keep in mind that a time dilation equal to the period of the clock leads to no measurable effect. Note that there is no need to measure the clock state. It is sufficient if the clock state is accessible in the operational sense.

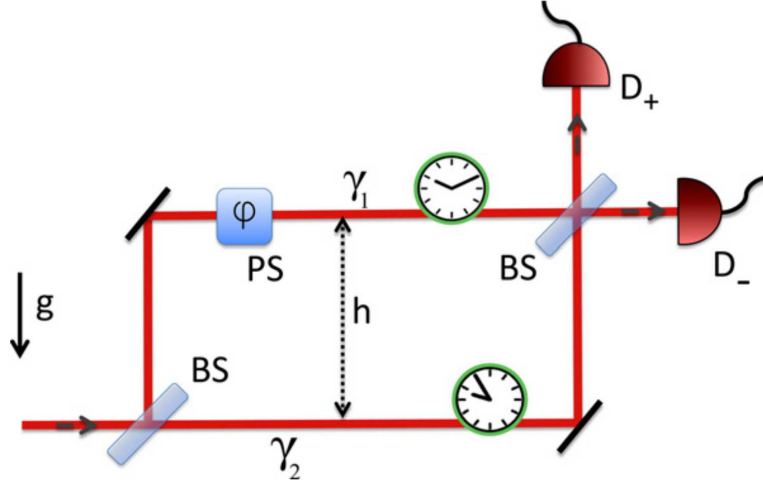


Figure 3: A Mach-Zehnder interferometer in the gravitational field. It consists of a two beam splitters (BS), a controllable phase shift (PS) and two detectors D_{\pm} . The two paths γ_1 and γ_2 are separated in height by h . (This figure is reproduced with permission from Zych et al. [1]).

The origin of this entanglement can be seen when considering the operators in the Schrödinger equation in coordinates where the particle is at rest. For the solution of the Schrödinger equation it holds:

$$i\hbar \frac{\partial}{\partial \tau} = H. \quad (34)$$

Here τ is the proper time (not to be confused with internal state labels τ_1 and τ_2) and H is the Hamiltonian of the internal clock degree of freedom. Since the particle is assumed to be a point particle the internal Hamiltonian is independent of any spatial coordinates, hence a transformation to the coordinate time t reads

$$i\hbar \frac{\partial}{\partial t} = \dot{\tau} H, \quad \dot{\tau} = \frac{d\tau}{dt}. \quad (35)$$

Since proper time τ of a world line x of a particle is defined as the parameter such that $-c^2 = g\left(\frac{dx}{d\tau}, \frac{dx}{d\tau}\right)$ for some metric g , one can find the flow $\dot{\tau}$ of the proper time with respect to the coordinate time t via:

$$-c^2 = g\left(\frac{dx}{d\tau}, \frac{dx}{d\tau}\right) = \left(\frac{dt}{d\tau}\right)^2 g\left(\frac{dx}{dt}, \frac{dx}{dt}\right) \Rightarrow \dot{\tau} = \frac{1}{c} \sqrt{-g\left(\frac{dx}{dt}, \frac{dx}{dt}\right)}. \quad (36)$$

In the case of the Schwarzschild metric the Newtonian potential $\phi(r) = -\frac{GM}{r}$ appears in the metric and therefore appears in $\dot{\tau}$. Thus in $\dot{\tau}H$ the coordinate r is coupled to the internal Hamiltonian H . Treating the coordinate r as an operator, it is this coupling which originates the entanglement between the internal clock state and the path of the particle.

While this describes interferometry with massive particles, photons are considered in a second paper [1]. In this case the position of the photon is analogous to the clock. While

the wave packets of the photon along the paths γ_1 and γ_2 (Fig. 3) would entirely overlap at the second beam splitter in absence of gravity, they are delayed in time with respect to each other when the interferometer is placed in a gravitational field due to time dilation which manifests itself as a Shapiro delay. For a stationary observer located at the second beam splitter this time dilation reads

$$\Delta\tau \approx \frac{lg h}{c^3} . \quad (\text{eq. (9) in [1]})$$

Here h and l are the dimensions of the interferometer (when considered as a rectangular shape in Fig. 3), g is the gravitational acceleration, and c is the speed of light. This clearly causes the visibility to drop since which-path information becomes available due to the different arrival times for each arm. For a photon with a Gaussian shape, a pulse width (coherence time) of σ , the visibility becomes

$$\mathcal{V} = e^{-\left(\frac{\Delta\tau}{t_{\perp}}\right)^2} , \quad (\text{eq. (13) in [1]})$$

where $t_{\perp} = \sqrt{8}\sigma$ is the so called precision of the clock (the time when the overlap of the two wave packets becomes smaller than $1/e$). Thus, the larger the time dilation $\Delta\tau$ and the shorter the coherence length σ of the photon, the larger is the drop in the visibility \mathcal{V} . To give a numerical example [1] assumes a femtosecond pulse. In order to get a drop in visibility of about $1/e$ the dimensions of the interferometer ($l \cdot h$) must be of the order of 10^3 km^2 . This is far beyond the reach of current technology.

In a more modest approach the interest can be focused on the relative phase shift instead of the time dilation (concerning both matter and photon interferometry). In contrast to time dilation a phase shift can also be explained with non-relativistic Newtonian gravity. There the phase shift occurs as a gravitational Aharonov-Bohm phase as the two arms of the interferometer guide through regions of different gravitational potential. Hence the experiment is no verification of an interplay between quantum mechanics and general relativity anymore. However, for a photon it can still be seen as a test of the mass-energy equivalence since a phase shift requires a coupling between the gravitational potential and the photon's rest mass (its energy divided by c^2).

3 Weak measurements

One way to amplify the small gravitational time dilation is to make use of the weak measurement formalism with postselections. In this section a general introduction to weak measurements is given. A connection to the particular interferometer experiment is established in ch. 4.

Weak measurement refers to a slightly modified von Neumann measurement scheme [10]. The coupling between a quantum system and a pointer (which is also treated as a quantum mechanical degree of freedom) is so weak, that an observation of the pointer state causes virtually no disturbance of the quantum system. It is a method to amplify the effects of weak couplings and to gain information about the evolution of a system without performing projective measurements. It was first introduced by Aharonov, Albert and Vaidman in 1988 [11]. The following is a introduction to the weak measurement scheme.

Let the initial quantum state be a product state $|I\rangle|\psi_I\rangle$ where $|I\rangle$ is the preselected state of the system and $|\psi_I\rangle$ is the state of the pointer. In the position representation one writes $\langle x|\psi_I\rangle = \psi_I(x)$. The weak coupling between system and pointer is modelled by the time-dependent Hamiltonian

$$H(t) = \lambda(t) A P , \quad (37)$$

where A is the observable of the system that couples to the momentum P of the pointer, and the coupling strength $\lambda(t)$ is such that its integral,

$$\int_{-\infty}^{\infty} \lambda(t) dt =: \delta , \quad (38)$$

is finite. This leads to the unitary evolution operator

$$U = e^{-\frac{i}{\hbar} \int H(t) dt} = e^{-\frac{i}{\hbar} \delta A P} . \quad (39)$$

Henceforth \hbar is set to 1 to improve the readability of the formulae. Applying U to the initial state creates the entanglement between the system and the pointer:

$$U|I\rangle|\psi_I\rangle = e^{-i\delta AP}|I\rangle|\psi_I\rangle = \sum_{k=0}^{\infty} \frac{(-i\delta)^k}{k!} A^k |I\rangle P^k |\psi_I\rangle = |I\rangle|\psi_I\rangle - i\delta A|I\rangle P|\psi_I\rangle + \dots . \quad (40)$$

Note that if the coupling constant δ is small, almost no information can be gained about the system by observing the pointer state. Performing a postselection on $\langle F|$ in the system degree of freedom results in a product state $|F\rangle|\psi_F\rangle$ where the state of the pointer is given by

$$|\psi_F\rangle = N \sum_{k=0}^{\infty} \frac{(-i\delta)^k}{k!} \langle F|A^k|I\rangle P^k |\psi_I\rangle , \quad (41)$$

in which N is a normalisation factor. Inserting identities $\mathbb{1} = \sum_l |a_l\rangle\langle a_l|$ in the basis where A is diagonal shows that the final pointer state is a superposition of shifted initial pointer

states

$$\begin{aligned}\psi_F(x) &= \langle x | \psi_F \rangle = N \sum_{k=0}^{\infty} \frac{(-i\delta)^k}{k!} \sum_l \langle F | A^k | a_l \rangle \langle a_l | I \rangle \langle x | P^k | \psi_I \rangle \\ &= N \sum_l \langle F | a_l \rangle \langle a_l | I \rangle \langle x | e^{-i\delta a_l P} | \psi_I \rangle = N \sum_l \langle F | a_l \rangle \langle a_l | I \rangle \psi_I(x - \delta a_l). \quad (42)\end{aligned}$$

Here it was used that $e^{-i\delta a_l P}$ is the translation operator.

The following approximation reveals an interesting and unexpected effect of these superpositions. By defining the so called weak value

$$A_W := \frac{\langle F | A | I \rangle}{\langle F | I \rangle}, \quad (43)$$

one can rewrite the final state of the pointer as

$$|\psi_F\rangle = N \langle F | I \rangle \left[\mathbb{1} - i\delta A_W P + \sum_{k=2}^{\infty} \frac{(-i\delta)^k}{k!} \frac{\langle F | A^k | I \rangle}{\langle F | I \rangle} P^k \right] |\psi_I\rangle. \quad (44)$$

Now the fact that δ is small comes into play. Assuming that δ is sufficiently small and $|\psi_I\rangle$ be such that the sum can be neglected for $k \geq 2$ (see below for the conditions), the final state of the pointer can be approximated like

$$|\psi_F\rangle \approx N \langle F | I \rangle [\mathbb{1} - i\delta A_W P] |\psi_I\rangle \approx e^{-i\delta A_W P} |\psi_I\rangle. \quad (45)$$

Since the unitary operator $e^{-i\delta A_W P}$ is the translation operator, the pointer is shifted by δA_W :

$$\psi_F(x) \approx \langle x | e^{-i\delta A_W P} | \psi_I \rangle = \psi_I(x - \delta A_W). \quad (46)$$

This shift can be of a disconcerting amount. The title "How the result of a measurement of a component of the spin of a spin-1/2 particle can turn out to be 100" of the pioneer paper [11] is an expression of that. So even if δ is small the shift δA_W can be very large by choosing the preselection $|I\rangle$ and the postselection $|F\rangle$ as nearly orthogonal states, leading to a large weak value (43). Note that this large shift can arise only for those states which survived the postselection. It is a consequence of the superposition of small shifts (42) where the complex amplitudes $\langle F | a_l \rangle \langle a_l | I \rangle$ cause non-trivial interference. Metaphorically speaking the postselection cancels all contributions in ψ_I except those which are centred around δA_W .

Note that the approximation (45) of (41) is critical. Remarkably in the original publication by Aharonov et al. [11] the conditions for this approximation to hold were erroneous. This was noticed by Duck, Stevenson and Sudarshan in 1989 [12] who gave the correct conditions. However Duck et al. calculated these conditions for the very special case of a pure real Gaussian pointer. Here these conditions are adapted for the case of a Gaussian pointer with a simple complex phase:

$$\psi_I(x) = \frac{1}{(2\pi\sigma^2)^{1/4}} \exp\left(-\frac{x^2}{4\sigma^2}\right) \exp(ip_0 x), \quad (47)$$

whose Fourier transform is

$$\tilde{\psi}_I(p) = \left(\frac{2\sigma^2}{\pi} \right)^{1/4} \exp \left(-\sigma^2(p - p_0)^2 \right). \quad (48)$$

Now the conditions for the approximation (45) of (41) read:

$$\frac{1}{\delta} \frac{1}{p_0 + \frac{1}{2\sigma}} \gg |A_W|, \quad (49)$$

$$\delta \left(p_0 + \frac{1}{2\sigma} \right) \ll \min_{k=2,3,\dots} \left| \frac{\langle F|A|I \rangle}{\langle F|A^k|I \rangle} \right|^{\frac{1}{k-1}}. \quad (50)$$

For the derivation see [12] and use (47) for the initial pointer state.

It is important to notice, however, that the amplification effect with large weak values A_W is at the cost of the probability to successfully postselect. This fact is underestimated in many introductions to weak measurement with postselections. To calculate the postselection probability the state operator ρ_S of the system is calculated by tracing out the pointer degree of freedom² after the weak interaction (40):

$$\begin{aligned} \rho_S &= \int \langle \mathbf{p} | U | I \rangle |\psi_I\rangle \langle I | \langle \psi_I | U^\dagger | \mathbf{p} \rangle d\mathbf{p} \\ &= \int \sum_{k,l=0}^{\infty} \frac{(-i\delta)^k}{k!} \frac{(i\delta)^l}{l!} A^k |I\rangle \langle I| A^l \langle \mathbf{p} | P^k | \psi_I \rangle \langle \psi_I | P^l | \mathbf{p} \rangle d\mathbf{p} \\ &= \int \sum_{k,l=0}^{\infty} \frac{(-i\delta)^k}{k!} \frac{(i\delta)^l}{l!} A^k |I\rangle \langle I| A^l \mathbf{p}^k \mathbf{p}^l |\langle \mathbf{p} | \psi_I \rangle|^2 d\mathbf{p} \\ &= \int e^{-i\delta p A} |I\rangle \langle I| e^{i\delta p A} |\tilde{\psi}_I(\mathbf{p})|^2 d\mathbf{p} \end{aligned} \quad (51)$$

The probability of a successful postselection is now given by

$$p = \langle F | \rho_S | F \rangle = \int |\langle F | e^{-i\delta p A} | I \rangle|^2 |\tilde{\psi}_I(\mathbf{p})|^2 d\mathbf{p} \quad (52)$$

This formula reveals that the postselection probability is the weighted integral of all transition probabilities $|\langle F | e^{-i\delta p A} | I \rangle|^2$ where the effective Hamiltonian $\delta p A$ of the system depends on the momentum \mathbf{p} . For small δ the leading term is just given by $|\langle F | I \rangle|^2$ which is proportional to the inverse of the magnitude squared of the weak value $1/|A_W|^2$. Thus:

²Since the symbol p denotes the postselection probability the momentum basis of the pointer is denoted by the symbol $|\mathbf{p}\rangle$.

The amplification effect and a successful postselection are inversely proportional.

Furthermore the last equation shows the unsurprising relation between the postselection probability p and the normalisation factor N ,

$$p = \frac{1}{N^2}, \quad (53)$$

by comparing (52) with an integration of the magnitude squared of (42).

If the weak value A_W (43) is complex the following two statements concerning the expectation values of the position $\langle X \rangle_F = \langle \psi_F | X | \psi_F \rangle$ and the momentum $\langle P \rangle_F = \langle \psi_F | P | \psi_F \rangle$ for the final pointer state hold:

$$\langle X \rangle_F = \langle X \rangle_I + \delta \operatorname{Re} A_W + \mathcal{O}(\delta^2), \quad (54)$$

$$\langle P \rangle_F = \langle P \rangle_I + 2 \delta \operatorname{Var}_I P \operatorname{Im} A_W + \mathcal{O}(\delta^2), \quad (55)$$

where $\operatorname{Var}_I P = \langle P^2 \rangle_I - \langle P \rangle_I^2$ is the variance of the pointer in the momentum degree of freedom in the initial state. This was pointed out by R. Josza [13]. Albeit the shift in the mean position is clear from the derivation above, the momentum shift requires explanation. Compared to the real part of the weak value which could be interpreted as a shift in the pointer position, the imaginary part can not be interpreted as creating a shift in the pointer's momentum since the interaction Hamiltonian (37) commutes with P . Hence there is no reason to expect any dynamics from the interaction like a shift in the momentum. However, the postselection originates some effective dynamics: The shift in the mean momentum can be interpreted as a kind of projection onto a fraction of the momentum distribution which was already present in the initial state of the pointer [14]. Therefore it depends on the variance $\operatorname{Var}_I P$ of the initial momentum distribution. Moreover, it turns out that the remaining factor, $2\delta \operatorname{Im} A_W$, is (to lowest order in δ) proportional to the logarithmic derivative³ of the transition probability $|\langle F | e^{-i\delta p A} | I \rangle|^2$ which also appears in the postselection probability (52). This can be seen in the following way:

$$\begin{aligned} \frac{\partial}{\partial p} \ln \left[|\langle F | e^{-i\delta p A} | I \rangle|^2 \right] &= -i\delta \left(\frac{\langle F | A e^{-i\delta p A} | I \rangle \langle I | e^{i\delta p A} | F \rangle}{\langle F | e^{-i\delta p A} | I \rangle \langle I | e^{i\delta p A} | F \rangle} - \frac{\langle F | e^{-i\delta p A} | I \rangle \langle I | A e^{i\delta p A} | F \rangle}{\langle F | e^{-i\delta p A} | I \rangle \langle I | e^{i\delta p A} | F \rangle} \right) \\ &= 2\delta \operatorname{Im} \left[\frac{\langle F | A e^{-i\delta p A} | I \rangle}{\langle F | e^{-i\delta p A} | I \rangle} \right] \\ &= 2\delta \operatorname{Im} A_W + \mathcal{O}(\delta^2). \end{aligned} \quad (56)$$

So the shift in the momentum is rather a postselection's product than a dynamical effect.

³the logarithmic derivative of a function f is simply defined by $(\ln f)' = f'/f$.

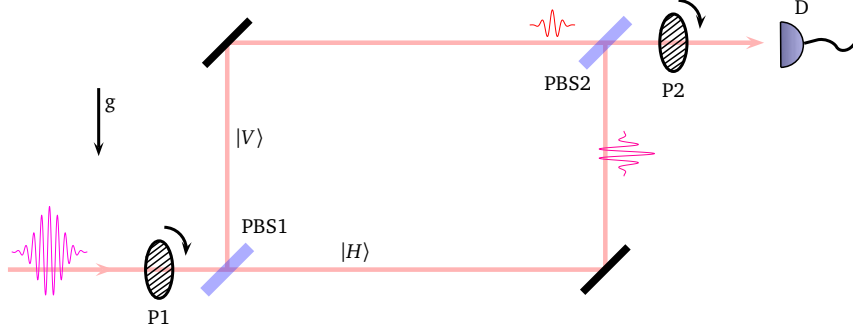


Figure 4: A Mach-Zehnder interferometer in the gravitational field with gravitational acceleration g . Two polariser (P1 and P2) preselect and postselect the polarisation of the photon. The polarising beam splitter (PBS1 and PBS2) divide and recombine the photon's path and correlate the path with the polarisation. The detector D represents a time of arrival measurement or a frequency detector.

4 Optical interferometer: Setup and theoretical approach

The setup, on which the analysis in this thesis is based, is slightly different from the original setup proposed by Zych et al. [1]. Instead of the visibility of the interference other effects of gravitational time dilation are proposed to uniquely prove the interplay between quantum mechanics and general relativity. The methods to measure these effects are presented in ch. 5. All of them are based on an interferometer experiment with preselections and postselections on single photons in a superposition of different paths in space-time.

4.1 Gravitational time dilation in a Mach-Zehnder interferometer

The setup is given by an optical Mach-Zehnder interferometer as in Fig. 4. The interferometer is build such that both arms have the same proper distance, where each consists of a horizontal part l and a vertical part h (see ch. 2.1 on p. 4 for an explanation of proper distance).

The polarisation of a single incident photon (see Fig. 4) is preselected by a polariser (P1) to be in the state

$$|I\rangle = \cos \alpha |H\rangle + \sin \alpha e^{i\chi} |V\rangle. \quad (57)$$

Here $|H\rangle$ and $|V\rangle$ form a basis in the Hilbert space over \mathbb{C}^2 and represent linear horizontal and linear vertical polarisation respectively. A polarising beam splitter (PBS1) which reflects vertical polarised light and transmits horizontal polarised light creates a superposition of two paths through different space-time regions. Which-path information is now encoded in the polarisation degree of freedom. Due to the Shapiro delay (or rather gravitational time dilation) the wave packet in the lower path needs more time to arrive at the second polarising beam splitter (PBS2) as measured by a stationary observer. This time dilation is gained only at the horizontal arms of the interferometer. Note that the gravitational redshift (occurring only in the vertical arms) affects both paths in the same way, so both

wave packets arrive with the same mean frequency at the second beam splitter. Since the photon travels on light-like geodesics the time dilation of the two wave packets is given by (see [1])

$$\Delta\tau \approx \frac{lg h}{c^3}, \quad (58)$$

as measured by a stationary observer sitting at the upper path. Here g is the gravitational acceleration and c is the speed of light. The approximation is valid as long as the arms of the interferometer, l and h , are short compared to the radius of the earth. The second polarising beam splitter (PBS2) which reflects horizontal polarised light and transmits vertical polarised light reunites both wave packets. For the stationary observer at the upper path the state between PBS2 and the second polariser P2 reads

$$|\Psi\rangle = \cos\alpha|H\rangle|\psi_{+\delta}\rangle + \sin\alpha e^{i\chi}|V\rangle|\psi_{-\delta}\rangle. \quad (59)$$

Here $\delta \equiv \Delta\tau/2$ and the photon states $|\psi_{\pm\delta}\rangle$ are defined as follows:

$$|\psi_{\pm\delta}\rangle = \int \tilde{\psi}(\omega) e^{\pm i\omega\delta} a_{\omega}^{\dagger} |0\rangle d\omega, \quad (60)$$

where a_{ω}^{\dagger} is a single photon creation operator acting on the vacuum $|0\rangle$, and $\tilde{\psi}(\omega)$ is the frequency distribution of the photon. The Fourier transform of $\tilde{\psi}(\omega)$ represents the temporal shape of the photon:

$$\psi(t) = \frac{1}{\sqrt{2\pi}} \int \tilde{\psi}(\omega) e^{i\omega t} d\omega. \quad (61)$$

Since vacuum is considered, one could also replace ω by $k = \omega/c$ and t by $x = ct$ to obtain the common notation with a_k^{\dagger} and a_x^{\dagger} . So the t in $\psi(t)$ does not refer to any kind of time evolution but $\psi(t)$ rather describes the shape of the photon at a given moment in time as observed by a stationary observer. The origin $t = 0$ is arbitrarily chosen as the peak of the pulse, see for example Fig. 5.

Note that the state $|\Psi\rangle$ is an entangled state since the horizontal polarised contribution is certainly correlated with the lagging wave packet and the vertical polarised contribution is certainly correlated with the wave packet ahead. The strength of the entanglement depends on the amount of the time dilation and the width of the wave packet. Reaching polariser P2 a postselection on

$$|F\rangle = \cos\beta|H\rangle + \sin\beta e^{i\varphi}|V\rangle \quad (62)$$

is performed. Thus the photon is finally in the product state $|F\rangle|\psi_F\rangle$ where its shape $|\psi_F\rangle$ depends on the preselection, the postselection, and the time dilation:

$$|\psi_F\rangle = N (\cos\alpha\cos\beta|\psi_{+\delta}\rangle + \sin\alpha\sin\beta e^{i(\chi-\varphi)}|\psi_{-\delta}\rangle). \quad (63)$$

The normalisation constant reads

$$N = (\cos^2\alpha\cos^2\beta + \sin^2\alpha\sin^2\beta + 2\cos\alpha\sin\alpha\cos\beta\sin\beta\cos(\chi-\varphi)\text{Re}\langle\psi_{+\delta}|\psi_{-\delta}\rangle)^{-1/2}. \quad (64)$$

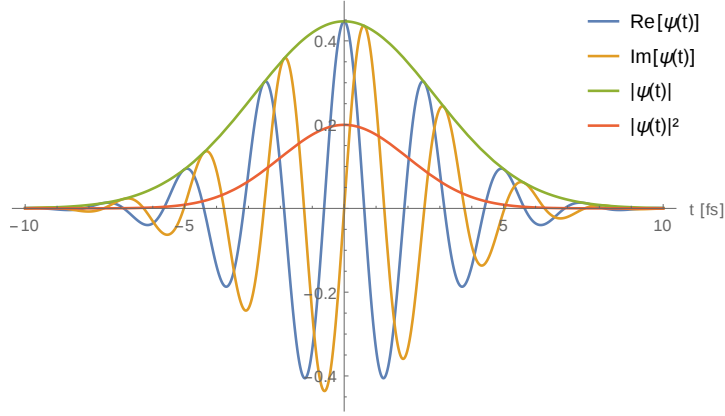


Figure 5: Example of a Gaussian pulse $\psi(t) = (2\pi\sigma^2)^{-1/4} \exp(-t^2/4\sigma^2) \exp(i\omega_0 t)$. The parameters are chosen as $\omega_0 = 2.5 \cdot 10^{15}$ Hz (red photon) and $\sigma = 2$ fs.

The shape of the photon or its frequency can be measured with the detector D which represents a time of arrival measurement or a frequency detector.

To establish a connection with the weak measurement formalism one can show that the state $|\Psi\rangle$ of eq. (59) can also be written as

$$|\Psi\rangle = e^{-i\delta AP} |I\rangle |\psi_{\delta=0}\rangle, \quad (65)$$

where

$$A = -|H\rangle\langle H| + |V\rangle\langle V| \quad (66)$$

and

$$P = -i \frac{\partial}{\partial t}. \quad (67)$$

This is exactly the same form as the state (40) in the introductory chapter of the weak measurements on p. 13. The following calculation proves that (65) is equal to (59):

$$\begin{aligned} e^{-i\delta AP} |I\rangle |\psi_{\delta=0}\rangle &= \sum_{k=0}^{\infty} \frac{(-i\delta)^k}{k!} A^k |I\rangle P^k |\psi_{\delta=0}\rangle \\ &= \sum_{k=0}^{\infty} \frac{(-i\delta)^k}{k!} (\cos \alpha A^k |H\rangle + \sin \alpha e^{i\chi} A^k |V\rangle) P^k |\psi_{\delta=0}\rangle \\ &= \sum_{k=0}^{\infty} \frac{(-i\delta)^k}{k!} (\cos \alpha (-1)^k |H\rangle + \sin \alpha e^{i\chi} (1)^k |V\rangle) P^k |\psi_{\delta=0}\rangle \quad (68) \\ &= \cos \alpha |H\rangle e^{i\delta P} |\psi_{\delta=0}\rangle + \sin \alpha e^{i\chi} |V\rangle e^{-i\delta P} |\psi_{\delta=0}\rangle \\ &= \cos \alpha |H\rangle |\psi_{+\delta}\rangle + \sin \alpha e^{i\chi} |V\rangle |\psi_{-\delta}\rangle. \end{aligned}$$

Note that the unitary operator $\exp(-i\delta AP)$ in (65) does not represent any physical dynamics taking place. It is merely a formal trick to apply the weak measurement formalism. At the same time this gives a formula for the weak value (43)

$$A_W = \frac{\langle F|A|I \rangle}{\langle F|I \rangle} = \frac{-\cos \alpha \cos \beta + \sin \alpha \sin \beta e^{i(\chi - \varphi)}}{\cos \alpha \cos \beta + \sin \alpha \sin \beta e^{i(\chi - \varphi)}} , \quad (69)$$

and also a formula for the postselection probability $p = 1/N^2$ (see eq. (53)), i.e. the probability that the photon passes P2:

$$p = \cos^2 \alpha \cos^2 \beta + \sin^2 \alpha \sin^2 \beta + \frac{1}{2} \sin 2\alpha \sin 2\beta \cos(\chi - \varphi) \text{Re} \langle \psi_{+\delta} | \psi_{-\delta} \rangle . \quad (70)$$

If the photon has a Gaussian envelope,

$$\psi(t) = \frac{1}{(2\pi\sigma^2)^{1/4}} \exp\left(-\frac{t^2}{4\sigma^2}\right) \exp(i\omega_0 t) , \quad (71)$$

where ω_0 denotes the mean frequency, the conditions (49) and (50) for the weak measurement formalism to be valid read in this case:

$$\frac{2}{\Delta\tau} \frac{1}{\omega_0 + \frac{1}{2\sigma}} \gg |A_W| , \quad (72)$$

$$\frac{\Delta\tau}{2} \left(\omega_0 + \frac{1}{2\sigma} \right) \ll \min_{k=2,3,\dots} \left| \frac{\langle F|A|I \rangle}{\langle F|A^k|I \rangle} \right|^{\frac{1}{k-1}} . \quad (73)$$

The shifts caused by the postselection described in (54) and (55) then occur in the mean arrival time and in the mean frequency respectively. If Δt denotes the shift in the mean arrival time and $\Delta\omega$ the shift in the mean frequency, they read:

$$\Delta t = \frac{\Delta\tau}{2} \text{Re} A_W + \mathcal{O}(\Delta\tau^2) , \quad (74)$$

$$\Delta\omega = \frac{\Delta\tau}{4\sigma^2} \text{Im} A_W + \mathcal{O}(\Delta\tau^2) . \quad (75)$$

4.2 Newtonian Limit

As mentioned at the end of ch. 2.3, no time dilation between the wave packets occurs if the effects of gravity are considered only in the Newtonian limit (NL). Since the coupling between the internal Hamiltonian and the gravitational potential is not present, the only effect of gravity is a relative gravitational scalar Aharonov-Bohm phase between the two paths in the interferometer. No entanglement occurs. The state between the second polarising beam splitter PBS2 and the postselection P2 is no longer given by (59) but reads

$$|\Psi^{\text{NL}}\rangle = \cos \alpha |H\rangle + \sin \alpha e^{i(\chi + \Phi)} |V\rangle , \quad (76)$$

where $\Phi = \Delta\tau\omega_0$ is the gravitational Aharonov-Bohm phase (see [1]). The temporal shape of the photon becomes unimportant since it is not affected. After a successful postselection the state is clearly in the pure state $|\psi_F^{\text{NL}}\rangle = |F\rangle$, instead of (63). Apparently the postselection probability will also change from (70) to

$$p^{\text{NL}} = \cos^2 \alpha \cos^2 \beta + \sin^2 \alpha \sin^2 \beta + \frac{1}{2} \sin 2\alpha \sin 2\beta \cos(\chi + \Phi - \varphi). \quad (77)$$

Since the aim of this thesis is to find more feasible methods which uniquely proof the existence of a gravitational time dilation, all methods have to be counterchecked in the Newtonian limit. This is due to the fact that an Aharonov-Bohm phase can have very similar effects than a time dilation if the time dilation is very small compared to the width of the photon pulse.

4.3 Alternative setup: Michelson-Morley interferometer

Alternatively to the Mach-Zehnder setup (Fig. 4) a Michelson-Morley type interferometer (Fig. 6) can be used. This setup might be easier to build and easier to handle since there are less elements. The interferometer arms have the same proper distance l like in the Mach-Zehnder case.

A polarising beam splitter again encodes the which-path information in the polarisation degree of freedom. To avoid that the photon returns at the source on its way back, a unitary operation W flips the polarisation in each arm. Since it acts on each wave packet twice W must be the square root of the NOT operator

$$W^2 \stackrel{!}{=} |H\rangle\langle V| \pm |V\rangle\langle H|, \quad (78)$$

which is, for example, given by

$$W = \frac{1}{\sqrt{2}} (|H\rangle\langle H| + |H\rangle\langle V| - |V\rangle\langle H| + |V\rangle\langle V|). \quad (79)$$

Experimentally this can be realised with $\lambda/4$ -plates or Faraday rotators. Like in the Mach-Zehnder case the Shapiro delay causes a time dilation between the two wave packets (see below for the calculation). After the postselection (at the polariser P2) the state reads like in the Mach-Zehnder case and is given by eq. (63) whereat the time dilation is here given by

$$\Delta\tau \approx \frac{gl^2}{c^3}. \quad (80)$$

This time dilation $\Delta\tau$ is calculated as follows: It is assumed that the horizontal path is approximately on the same radial coordinate R in the Schwarzschild metric (1). While the angle θ changes by an amount of l/R all other spatial coordinates stay constant. Thus the length of this arm can trivially be defined via

$$l = \int_0^{l/R} R d\theta. \quad (81)$$

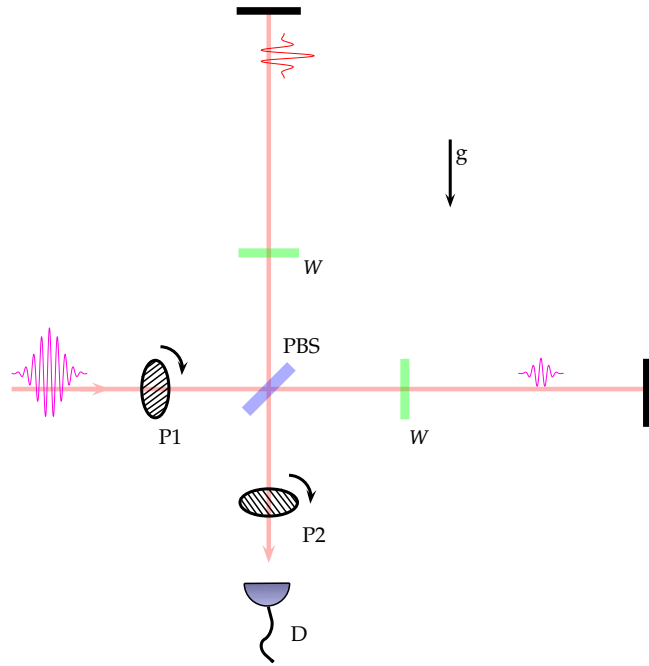


Figure 6: A Michelson-Morley interferometer in the gravitational field with gravitational acceleration g . Two polarisers (P1 and P2) preselect and postselect the polarisation of the photon. The polarising beam splitter (PBS) divides and recombines the photon's path and correlates the path with the polarisation. The unitary transformation W^2 (e.g. a $\lambda/4$ -plate or a Faraday rotator) flips the photon's polarisation in order to reach detector D. The detector D represents a time of arrival measurement or a frequency detector.

On the other hand the vertical path is described by a world line with fixed angular coordinates and variable radial coordinate going from R to $R + \Delta R$. Since l is already fixed ΔR is defined by

$$l = \int_R^{R+\Delta R} \frac{1}{\sqrt{1 - \frac{2GM}{c^2 r}}} dr. \quad (82)$$

The elapsed coordinate time for the horizontal world line is

$$\begin{aligned} \Delta t_H &= \frac{1}{c} \frac{1}{\sqrt{1 - \frac{2GM}{c^2 R}}} \int_0^{l/R} R d\theta = \frac{1}{c} \frac{l}{\sqrt{1 - \frac{2GM}{c^2 R}}} \\ &= \frac{1}{c} \frac{1}{\sqrt{1 - \frac{2GM}{c^2 R}}} \int_R^{R+\Delta R} \frac{1}{\sqrt{1 - \frac{2GM}{c^2 r}}} dr, \end{aligned} \quad (83)$$

and for the vertical (radial) world line it is

$$\Delta t_V = \frac{1}{c} \int_R^{R+\Delta R} \frac{1}{1 - \frac{2GM}{c^2 r}} dr. \quad (84)$$

An expansion of $\Delta t_H - \Delta t_V$ for small $\Delta R/R$ reveals the time dilation in the coordinate time:

$$\Delta t_H - \Delta t_V = \frac{GM}{2c^3} \frac{1}{\left(1 - \frac{2GM}{c^2 R}\right)^2} \left(\frac{\Delta R}{R}\right)^2 + \mathcal{O}\left(\frac{\Delta R}{R}\right)^3. \quad (85)$$

For a stationary observer at R this difference in coordinate time corresponds to a measured proper time interval of

$$\frac{\Delta \tau}{2} = \sqrt{1 - \frac{2GM}{c^2 R}} (\Delta t_H - \Delta t_V) = \frac{GM}{2c^3} \frac{1}{\left(1 - \frac{2GM}{c^2 R}\right)^{3/4}} \left(\frac{\Delta R}{R}\right)^2 + \mathcal{O}\left(\frac{\Delta R}{R}\right)^3. \quad (86)$$

In order to express this proper time interval in terms of l instead of ΔR , one can expand the relation (82) between l and ΔR to lowest order,

$$l = \frac{R}{\sqrt{1 - \frac{2GM}{c^2 R}}} \frac{\Delta R}{R} + \mathcal{O}\left(\frac{\Delta R}{R}\right)^2, \quad (87)$$

to get the approximation

$$\frac{\Delta \tau}{2} \approx \frac{gl^2}{2c^3} \quad (88)$$

for (86), where $g = \frac{GM}{R^2}$. Since the wave packets travel both world lines twice the overall time dilation results in (80).

5 Methods and results

In this section five methods are presented to achieve a more feasible parameter range for real experiments. The great challenge in this respect is mainly the fact, that the time dilation $\Delta\tau$ (see eq. (58) on p. 18) is very small if the dimensions of the used interferometer are of conventional order. An interferometer which encloses a surface of $A = l \cdot h = 100 \text{ m}^2$ leads to a time dilation of about $\Delta\tau \approx 3.6 \cdot 10^{-23} \text{ s}$ when placed vertically on Earth. On the other hand a time dilation in the range of attoseconds (10^{-18} s) requires a surface of about $A \approx 2.7 \text{ km}^2$ for a quadratic interferometer which corresponds to an arm length of about 1.6 km. Thus the assumption that the time dilation is in the sub-pulse-width regime of the used photons is reasonable and reflects the constant challenge of this thesis.

The quantity $\Delta\tau/\sigma$, where σ is the pulse width, represents a measure for the accessibility of the time dilation. Hence very short pulses are advisable. However, since the pulse width is related to the frequency distribution, the restriction to optical photons ($\omega_0 \sim 10^{15} \text{ Hz}$) is, at the same time, a restriction to pulse widths of about femtoseconds or broader. To see this, consider the following naive and rough estimation: If the pulse has a width of σ the "electric field needs the chance to oscillate at least once" during σ , hence $\sigma > 2\pi/\omega_0 = 6.28 \text{ fs}$. Another way to get a similar inequality is based on the assumption, that the pulse has a Gaussian shape like in (71) with a pulse width σ . From a simple Fourier transformation follows that the spectral bandwidth is given by $1/2\sigma$. In order to avoid nonphysical negative frequency contributions the mean frequency ω_0 should be much larger than the spectral bandwidth, so $\omega_0 \gg 1/2\sigma$. This is equivalent to $\sigma \gg 1/2\omega_0 = 0.5 \text{ fs}$. For simplicity, henceforth, the lower bound of the pulse width is given by

$$\sigma \geq 1/\omega_0 . \quad (89)$$

For a more detailed discussion see [15].

Moreover this states that the usage of, e.g., attosecond photons requires frequencies of at least 10^{18} Hz . This is already in the soft X-ray regime, so the setup can no longer be based on optical devices.

In method 1 the formalism of weak measurements is used to predict an amplified shift in the mean frequency and in the mean arrival time of the single photons in dependence of the gravitational time dilation. These shifts are consequences of the weak measurement with postselections in the polarisation afterwards. Method 2 presents a way to amplify phase shifts with postselections and was inspired by the previous method. However, instead of the gravitational time dilation only the gravitational phase shift or rather the mass-energy equivalence for single photons can be tested. In method 3 it is shown how the postselection probability depends on the shape of the photon or rather how it can be amplified by using additional controllable time dilations caused by positioner elements. This positioner elements can vary the effective difference in the arm length in the subnanometer regime. Like the first method it probes the gravitational time dilation directly. Method 4 shows how the gravitational phase shift can deform the shape of the photon: A double-humped shape can be created or destroyed in dependence of the gravitational phase shift. In the last method, a certain frequency of the photon is cut out due to destructive interference in dependence of

the gravitational phase shift. Sending these photons through a gas which absorbs photons with a certain frequency could reveal which frequency is cut out.

As pointed out in 2.3 it is necessary to distinguish the case of direct consequences of the gravitational time dilation from effects which result from the gravitational phase shift: Since the latter can be explained via a gravitational scalar Aharonov-Bohm phase where the photon's rest mass (its energy divided by c^2) couples to the Newtonian potential, it is no verification of a gravitational time dilation. However, measuring the gravitational phase shift could serve as a test to verify the mass-energy equivalence for single photons.

5.1 Method 1: Amplified shifts of the mean frequency and mean arrival time

In this method the position of the photon is interpreted as the pointer of a weak measurement. The connection between the experiment considered here and weak measurements was already established in ch. 4.1 on p. 19: The postselection causes shifts in the mean arrival time and in the mean frequency of the photon, see eq. (74) and (75). Therefore detector D in Fig. 4 or 6 is now considered as measuring either the arrival time or the frequency of the incoming photons. Since these shifts require an actual time dilation, no shifts occur in the Newtonian limit. This method is essentially based on [16]⁴.

However, the relevant quantities are not the absolute shifts, but rather the shifts in relation to the width of the particular wave function (i.e. the broadness of the pulse or the bandwidth). For example, the broader the bandwidth the more difficult it becomes to detect a shift in the mean frequency. Since, for a Gaussian (71), the width in the time domain is σ and the width in the frequency domain is $1/2\sigma$, the two relative shifts are defined as follows. For the relative shift in the arrival time one defines

$$\kappa_t := \frac{\Delta t}{\sigma} = \frac{1}{2} \frac{\Delta \tau}{\sigma} \text{Re}A_W, \quad (90)$$

and the definition of the relative shift in the mean frequency reads

$$\kappa_\omega := \frac{\Delta \omega}{1/2\sigma} = \frac{1}{2} \frac{\Delta \tau}{\sigma} \text{Im}A_W. \quad (91)$$

So both relative shifts depend on the ratio between the gravitational time dilation $\Delta \tau$ and the pulse width σ in the same way. The only difference is that the former is amplified by the real part of the weak value whereas the latter is amplified by the imaginary part of the weak value. Note that the weak value can not be made arbitrarily large. So for both κ_t and κ_ω a general bound can be derived, using the condition (72):

$$|\kappa_t| = \frac{1}{2} \frac{\Delta \tau}{\sigma} |\text{Re}A_W| \leq \frac{1}{2} \frac{\Delta \tau}{\sigma} |A_W| \ll \frac{1}{2} \frac{\Delta \tau}{\sigma} \frac{2}{\Delta \tau} \frac{1}{\omega_0 + 1/2\sigma} = \frac{1}{\sigma \omega_0 + 1/2}. \quad (92)$$

The same holds for κ_ω , hence the two bounds are

$$|\kappa_x| \ll \frac{1}{\sigma \omega_0 + 1/2}, \quad x = t, \omega. \quad (93)$$

Note that since $\sigma \geq 1/\omega_0$, which is the necessary condition (89) for producible photons, the product $\sigma \omega_0 \geq 1$ is indeed the crucial contribution of the bound. If, for example, green picosecond photons ($\omega_0 = 3.5 \cdot 10^{15}$ Hz, $\sigma = 10^{-12}$ s) are considered, the bound becomes $\kappa_x \ll 2.9 \cdot 10^{-4} = 0.029\%$ which is unpromising. On the other hand for red femtosecond photons ($\omega_0 = 5 \cdot 10^{15}$ Hz, $\sigma = 10^{-15}$ s) the bound looks more promising: $\kappa_x \ll 0.18 = 18\%$.

⁴Even though the title of [16] refers to measuring phase shifts, they actually propose a method to measure time dilations.

To create large real and imaginary weak values A_W , it is necessary to choose the postselected state as orthogonal as possible to the preselected state without violating the condition (72).

Let ε serve as the parameter to vary the amount of the weak value:

- (a) Intending a shift in the mean arrival time, the preselection and postselection are chosen by $\alpha = \frac{\pi}{4}$, $\chi = 0$, $\beta = \frac{3\pi}{4} - \varepsilon$, $\varphi = 0$. Hence the weak value becomes

$$A_W = \cot \varepsilon \quad \Rightarrow \quad \text{Re}A_W = \cot \varepsilon, \quad (94)$$

and for the postselection probability one obtains

$$p = \frac{1 - \cos(2\varepsilon) \cos(\omega_0 \Delta \tau) e^{-\frac{\Delta \tau^2}{8\sigma^2}}}{2}. \quad (95)$$

- (b) On the other hand, intending a shift in the mean frequency, the preselection and postselection are chosen by $\alpha = \frac{\pi}{4}$, $\chi = 0$, $\beta = \frac{3\pi}{4}$, $\varphi = 2\varepsilon$. Hence the weak value becomes

$$A_W = i \cot \varepsilon \quad \Rightarrow \quad \text{Im}A_W = \cot \varepsilon, \quad (96)$$

and the postselection probability gets the same form as in case (a).

Since the postselection probability is equal for both cases and furthermore $\text{Re}A_W$ from case (a) equals $\text{Im}A_W$ from case (b), the calculations are henceforth carried out by the general form

$$\kappa_x = \frac{1}{2} \frac{\Delta \tau}{\sigma} \cot \varepsilon, \quad (97)$$

where x stands for t or ω . As also the postselection probability equals for both cases (a) and (b) one finds the analytical relation between p and κ_x for both cases:

$$p(\kappa_x) = \frac{1 - \cos\left(2 \cot^{-1}\left(2 \frac{\sigma}{\Delta \tau} \kappa_x\right)\right) \cos(\omega_0 \Delta \tau) e^{-\frac{\Delta \tau^2}{8\sigma^2}}}{2}. \quad (98)$$

An expansion for small $\Delta \tau$ reveals

$$p(\kappa_x) = \frac{1}{4} \left[\frac{1}{\sigma^2} \left(\frac{1}{4} + \frac{1}{\kappa_x^2} \right) + \omega_0^2 \right] \Delta \tau^2 + \mathcal{O}(\Delta \tau^4). \quad (99)$$

Since from (93) one gets $\kappa_x \ll 2$ and $\kappa_x \ll 1/\sigma \omega_0$ one can write the last equation as:

$$p(\kappa_x) = \frac{1}{4} \frac{\Delta \tau^2}{\sigma^2 \kappa_x^2} + \mathcal{O}\left(\frac{\Delta \tau^2}{\sigma^2} + \omega_0^2 \Delta \tau^2\right). \quad (100)$$

In Fig. 7 several plots of the postselection probability (98) in dependence of κ_x are shown

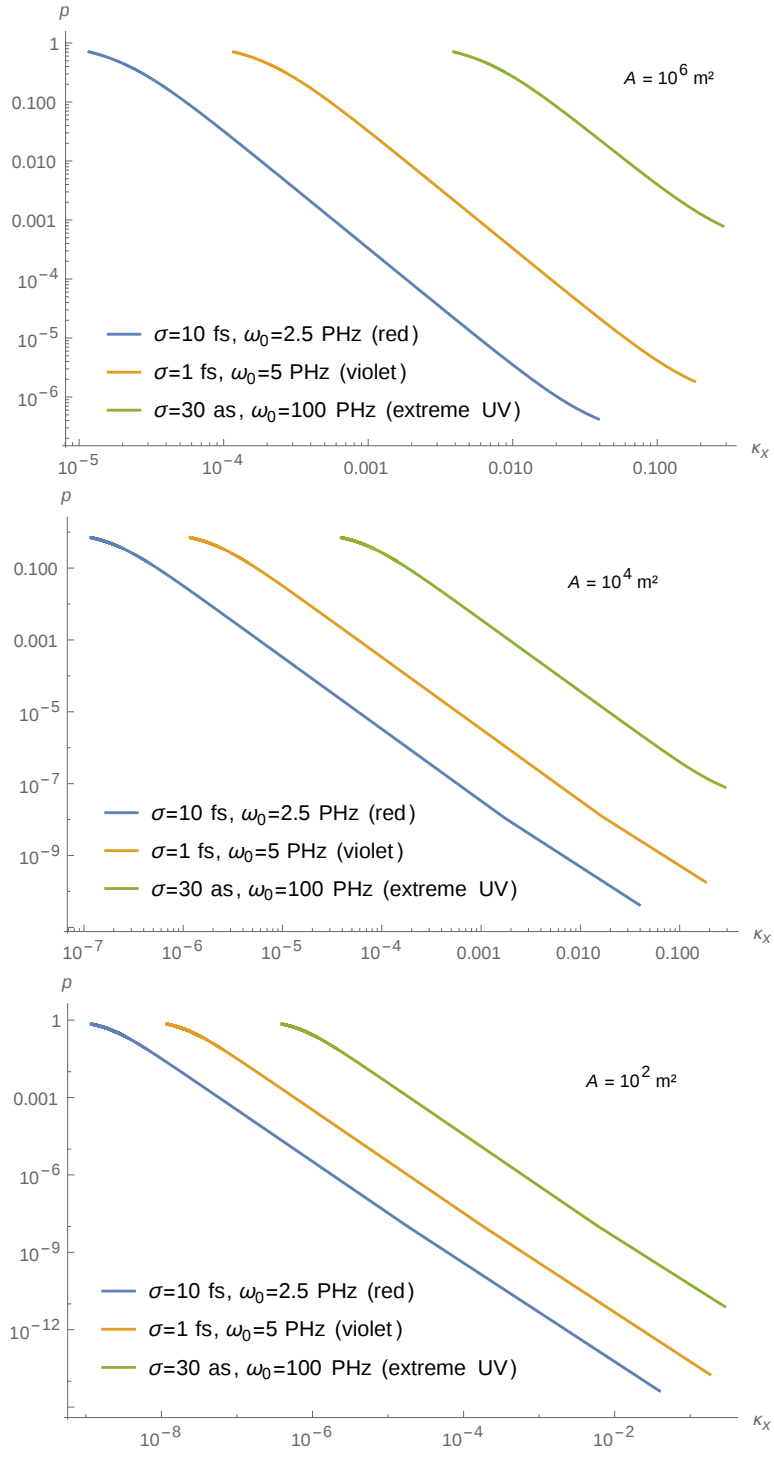


Figure 7: Plots of the postselection probability (98) in dependence of the relative shift κ_x due to the postselection. κ_x refers to both the relative shift κ_t in the mean arrival time from (90) and to the relative shift κ_ω in the mean frequency from (91) if the preselection and postselection was chose as in case (a) or case (b) on p. 28.

for different pulse widths and different cross sections of the interferometer.

A numerical example is instructive: 10^9 red femtosecond photons per second ($\omega_0 = 2.5 \cdot 10^{15}$ Hz, $\sigma = 1$ fs) are sent through the interferometer with a surface of about $A = \Delta\tau c^3/g = 10^4 \text{ m}^2$. In order to have at least 10 surviving photons per second after the postselection one can admit the postselection probability to be $p = 10^{-8}$. This results in a relative shift of $\kappa_x = 0.18\%$. Thus, e.g., the mean frequency of the surviving photons is shifted by $\omega_0 \kappa_x = 4.95$ THz. Apart from the fact that the cross section of the interferometer is still too large, these parameters are in the feasible regime. Note that a surface of 10^4 m^2 is five orders of magnitude smaller than 10^3 km^2 as suggested in [1].

5.2 Method 2: Phase amplification via postselections

If only the gravitational Aharonov-Bohm phase $\Phi = \omega_0 \Delta\tau$ (see [1]) is of interest, the method presented in this chapter constitutes in analogy to weak measurements an opportunity to amplify this phase via postselections in the polarisation degree of freedom⁵. In the case when only the existence of the phase shift is of interest (instead of a test of the equivalence principle for single photons), a coherent laser beam with a mean frequency of ω_0 can be used instead of single photons. A gravitational time dilation $\Delta\tau$ then manifests itself only as a phase shift. The setup is shown in Fig. 8. It is basically the same setup as introduced in ch. 4 (see Fig. 4 or 6). But before the beam reaches the gravitationally influenced interferometer it is splitted by a preceding beam splitter into two spatial modes $|0\rangle$ and $|1\rangle$. Only the former mode guides the beam through the gravitational interferometer where the gravitational Aharonov-Bohm phase Φ occurs in the polarisation degree of freedom. Next a postselection on an almost orthogonal polarisation is performed in both modes $|0\rangle$ and $|1\rangle$. This postselection approximately establishes an amplified relative phase Φ/ε between the two modes where ε is the parameter to vary deviations from an orthogonal postselection. The postselection probability is approximately given by ε^2 .

The physical process in the setup from Fig. 8 is as follows: The first polariser P1 pre-selects linear diagonal polarised photons, $|H\rangle + |V\rangle$, coming from below. The first beam splitter BS1 splits the beam into a part which travels through the gravitationally influenced interferometer (dashed box) whereas the other part propagates freely. A relative phase ξ is established between the modes $|0\rangle$ and $|1\rangle$ by a phase shift element. Inside the gravitationally influenced interferometer the vertical and horizontal polarised parts of the beam experience the relative Aharonov-Bohm phase Φ as described in ch. 4. For simplicity unnormalised states are used to describe the physical process in the setup: Inside the dashed box (which contains the part of the interferometer which is placed into the gravitational field) only a relative Aharonov-Bohm phase Φ occurs between $|H\rangle$ and $|V\rangle$.

$$\begin{aligned}
 (|H\rangle + |V\rangle)|1\rangle &\xrightarrow{\text{BS1}} (|H\rangle + |V\rangle)(|0\rangle + i|1\rangle) \\
 &\xrightarrow{\text{dashed box}} \left(e^{-i\frac{\Phi}{2}}|H\rangle + e^{i\frac{\Phi}{2}}|V\rangle\right)|0\rangle + (|H\rangle + |V\rangle)i|1\rangle \\
 &\xrightarrow{\text{phase } \xi} \left(e^{-i\frac{\Phi}{2}}|H\rangle + e^{i\frac{\Phi}{2}}|V\rangle\right)|0\rangle + (|H\rangle + |V\rangle)ie^{i\xi}|1\rangle. \quad (101)
 \end{aligned}$$

Next a postselection on

$$|F\rangle = \cos\left(\frac{3\pi}{4} + \varepsilon\right)|H\rangle + \sin\left(\frac{3\pi}{4} + \varepsilon\right)|V\rangle \quad (102)$$

is performed in both modes $|0\rangle$ and $|1\rangle$ when the beams pass P2:

$$\begin{aligned}
 &\xrightarrow{\text{P2}} \left(\cos\left(\frac{3\pi}{4} + \varepsilon\right)e^{-i\frac{\Phi}{2}} + \sin\left(\frac{3\pi}{4} + \varepsilon\right)e^{i\frac{\Phi}{2}}\right)|0\rangle + \left(\cos\left(\frac{3\pi}{4} + \varepsilon\right) + \sin\left(\frac{3\pi}{4} + \varepsilon\right)\right)ie^{i\xi}|1\rangle \\
 &= \left(i\cos\varepsilon\sin\frac{\Phi}{2} - \sin\varepsilon\cos\frac{\Phi}{2}\right)|0\rangle - ie^{i\xi}\sin\varepsilon|1\rangle. \quad (103)
 \end{aligned}$$

⁵This method is inspired by private communication between Li Li, Ľaslav Brukner and the author of this thesis.

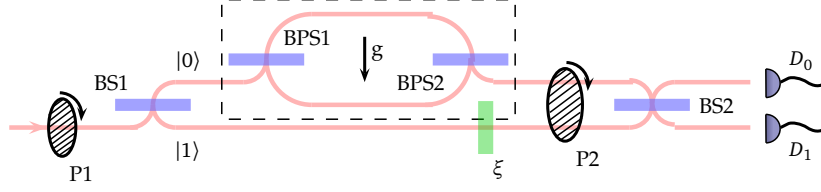


Figure 8: Setup for an amplification of the gravitational Aharonov-Bohm phase. The interferometer in the dashed box is similar to the two setups introduced in ch. 4: The two arms which guide the beam through regions of different gravitational potential, experience a relative Aharonov-Bohm phase. The two additional beam splitters BS1 and BS2 split and combine the beam into two spatial modes $|0\rangle$ and $|1\rangle$. The preselection and postselection which leads to the amplification effect is performed with the polarisers P1 and P2. The lower mode gains a controllable phase shift ξ . The detector D_0 and D_1 measure the intensity of the outgoing beams.

At last the second beam splitter provides interference between the two spatial modes:

$$\begin{aligned} & \xrightarrow{\text{BS2}} \left(i \cos \varepsilon \sin \frac{\Phi}{2} - \sin \varepsilon \cos \frac{\Phi}{2} \right) (i|0\rangle + |1\rangle) - e^{i\xi} \sin \varepsilon (i|0\rangle - |1\rangle) \\ &= \left(i \cos \varepsilon \sin \frac{\Phi}{2} - \sin \varepsilon \cos \frac{\Phi}{2} - e^{i\xi} \sin \varepsilon \right) i|0\rangle + \left(i \cos \varepsilon \sin \frac{\Phi}{2} - \sin \varepsilon \cos \frac{\Phi}{2} + e^{i\xi} \sin \varepsilon \right) |1\rangle. \end{aligned} \quad (104)$$

In order to calculate the detection probabilities (or the beam intensities in the case of a laser beam), this resulting state which reaches the two detectors D_0 and D_1 is normalised to 1:

$$|\Psi\rangle = \frac{(i \cot \varepsilon \sin \frac{\Phi}{2} - \cos \frac{\Phi}{2} - e^{i\xi}) i|0\rangle + (i \cot \varepsilon \sin \frac{\Phi}{2} - \cos \frac{\Phi}{2} + e^{i\xi}) |1\rangle}{\sqrt{2 \left(2 + \sin^2 \frac{\Phi}{2} (\cot^2 \varepsilon - 1) \right)}}. \quad (105)$$

Here the amplification effect is already apparent. If Φ is small, the cosine terms are close to 1 whereas the small sine terms are amplified by $\cot \varepsilon$. Note that $\cot \varepsilon \rightarrow \infty$ if $\varepsilon \rightarrow 0$. The detection probabilities P_0 and P_1 (beam intensities) of the detectors D_0 and D_1 read:

$$P_0 = \langle 0|\Psi|0\rangle = \frac{1}{2} - \frac{\cot \varepsilon \sin \frac{\Phi}{2} \sin \xi - \cos \frac{\Phi}{2} \cos \xi}{2 + \sin^2 \frac{\Phi}{2} (\cot^2 \varepsilon - 1)}, \quad (106)$$

$$P_1 = \langle 1|\Psi|1\rangle = \frac{1}{2} + \frac{\cot \varepsilon \sin \frac{\Phi}{2} \sin \xi - \cos \frac{\Phi}{2} \cos \xi}{2 + \sin^2 \frac{\Phi}{2} (\cot^2 \varepsilon - 1)}. \quad (107)$$

Since the gravitational Aharonov-Bohm phase Φ is in all practical considerations very small, an expansion of the detection probabilities is appropriate. For $\xi = \frac{\pi}{2}$ and $0 < \Phi \ll \varepsilon < 1$ the expansion reveals the amplification effect $\Phi \rightarrow \Phi/\varepsilon$:

$$P_0 = \frac{1}{2} \left(1 - \frac{\Phi}{2\varepsilon} \right) + \mathcal{O}(\varepsilon\Phi), \quad (108)$$

$$P_1 = \frac{1}{2} \left(1 + \frac{\Phi}{2\varepsilon} \right) + \mathcal{O}(\varepsilon\Phi). \quad (109)$$

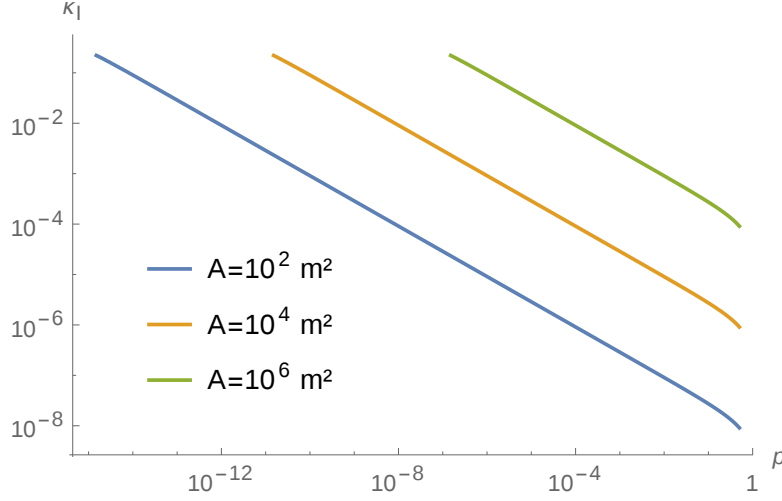


Figure 9: Plots of the relative change in the intensity κ_I at the detectors D_0 and D_1 in dependence of the loss of the beam p at P2, see eq. (114). The laser has a mean frequency of $\omega_0 = 10^{15}$ Hz. The different plots are based on different surfaces A of the gravitationally influenced part of the interferometer. The relation to the Aharonov-Bohm phase is given by $\Phi = \omega_0 \Delta \tau = \omega_0 \frac{Ag}{c^3}$.

However, the probability of a successful postselection (loss of the beam intensity in the case of a laser beam) must not be ignored. The state in the polarisation degree of freedom ρ_{Pol} is calculated by tracing out the path degree of freedom of the state (101) right before the beam arrives at P2:

$$\rho_{\text{Pol}} = \frac{1}{2} \left(|H\rangle\langle H| + \frac{1}{2}|H\rangle\langle V| (1 + e^{-i\Phi}) + \frac{1}{2}|V\rangle\langle H| (1 + e^{i\Phi}) + |V\rangle\langle V| \right). \quad (110)$$

Hence the postselection probability p reads:

$$p = \langle F | \rho_{\text{Pol}} | F \rangle = \frac{1}{2} \left(1 - \cos(2\varepsilon) \frac{1 + \cos \Phi}{2} \right). \quad (111)$$

Considering again the expansion for $0 < \Phi \ll \varepsilon < 1$, one gets:

$$p = \varepsilon^2 + \mathcal{O}(\Phi^2). \quad (112)$$

Now the quantity of interest is the relative change of the beam intensities in the detectors due to the gravitational Aharonov-Bohm phase Φ in dependence of the postselection probability p (loss of the beam at P2). Accordingly the relative change of the beam intensities is defined as:

$$\kappa_I := \left| \frac{P_0(\Phi) - P_0(0)}{P_0(0)} \right| = \left| \frac{P_1(\Phi) - P_1(0)}{P_1(0)} \right| = \frac{2 \cot \varepsilon \sin \frac{\Phi}{2}}{2 + \sin^2 \frac{\Phi}{2} (\cot^2 \varepsilon - 1)}. \quad (113)$$

Note that the choice $\xi = \frac{\pi}{2}$ is still assumed. Replacing ε with the postselection probability p (by solving (111) for ε) yields the desired dependency between κ_I and p :

$$\kappa_I(p) = \frac{2 \cot\left(\frac{1}{2} \arccos\left(2 \frac{1-2p}{1+\cos\Phi}\right)\right) \sin \frac{\Phi}{2}}{2 + \sin^2 \frac{\Phi}{2} \left(\cot^2\left(\frac{1}{2} \arccos\left(2 \frac{1-2p}{1+\cos\Phi}\right)\right) - 1\right)}. \quad (114)$$

For $0 < \Phi \ll p < 1$ an expansion reads:

$$\kappa_I(p) = \frac{\Phi}{2\sqrt{p}} + \mathcal{O}(\sqrt{p}\Phi). \quad (115)$$

In Fig. 9 examples of the function $\kappa_I(p)$ from (114) are plotted for a laser with $\omega_0 = 10^{15}$ Hz and several surfaces A of the gravitationally influenced interferometer. Note that $\Phi = \omega_0 \Delta \tau = \omega_0 \frac{Ag}{c^3}$.

One could think that introducing an additional controllable phase on top of the Aharonov-Bohm phase could improve the sensitivity of κ_I in dependence of Φ . However, the slope of κ_I as a function of Φ is already maximal at $\Phi = 0$ as long as $|\varepsilon| < 0.866$:

$$\frac{d^2}{d^2\Phi} \kappa_I|_{\Phi=0} = 0, \quad \frac{d^3}{d^3\Phi} \kappa_I|_{\Phi=0} = \frac{2 - 3 \cot^2 \varepsilon}{6} \cot \varepsilon < 0. \quad (116)$$

Since, for all practical purposes, $|\varepsilon| < 0.866$ is no restriction, the relative change of the beam intensities κ_I is already maximal sensitive if Φ is small.

Concluding this section a set of parameters is given that might be suitable for an experiment: Let the surface of the gravitationally influenced interferometer be $A = 10^4 \text{ m}^2$. Photons or a laser beam with a mean frequency of $\omega_0 = 10^{15}$ Hz are used and the desired relative change of the detection probabilities / intensities due to the gravitational Aharonov-Bohm phase be 1%, hence $k_I = 0.01$. Hence one needs $\varepsilon \approx 1.8 \cdot 10^{-4}$. Conducting the experiment without gravitational influence the loss at P2 is $p \approx 3.2 \cdot 10^{-8}$. Thus the photon flux / laser power needs to be sufficiently high. The detectors D_0 and D_1 will measure exactly the same intensity since $P_0 = P_1 = \frac{1}{2}$. If now the interferometer is placed into the gravitational field the intensities at D_0 and D_1 will change by $\kappa_I = 1\%$ since the Aharonov-Bohm phase $\Phi \approx 3.6 \cdot 10^{-6}$ occurs:

$$P_0 \approx \frac{1}{2} \left(1 - \frac{3.6 \cdot 10^{-6}}{2 \cdot 1.8 \cdot 10^{-4}}\right) = \frac{1}{2} (1 - 10^{-2}), \quad (117)$$

$$P_1 \approx \frac{1}{2} \left(1 + \frac{3.6 \cdot 10^{-6}}{2 \cdot 1.8 \cdot 10^{-4}}\right) = \frac{1}{2} (1 + 10^{-2}). \quad (118)$$

Using laser light instead of single photons, even smaller interferometers could be used since small postselection probabilities can be compensated by high laser intensities.

5.3 Method 3: Additional controllable time delay

This method is similar to the initial experimental suggestion by Zych et al. [1]. The postselection probability which depends on the time dilation is measured by counting the number of photons which arrive in the detector D. Therefore it could possibly be used as a measure of the time dilation. The postselection is chosen such that this probability is equal to the probability to measure a photon in detector D_- (see Fig. 3) in the original setup suggested in [1]. Thus this method can easily be adapted to the original proposal. However, other pulse shapes and the effect of an additional controllable time delay are considered here.

The preselected $|I\rangle$ and the postselected state $|F\rangle$ are chosen as orthogonal states:

$$|I\rangle = \frac{1}{\sqrt{2}}(|H\rangle + |V\rangle), \quad (119)$$

$$|F\rangle = \frac{1}{\sqrt{2}}(|H\rangle - |V\rangle). \quad (120)$$

This corresponds to a choice of $\alpha = -\beta = \pi/4$, $\chi = \varphi = 0$. The probability of a successful postselection is then given by (70):

$$p = \frac{1 - \text{Re}\langle\psi_{+\delta}|\psi_{-\delta}\rangle}{2}. \quad (121)$$

Consider now a photon with a Gaussian shape (71),

$$\psi(t) = \frac{1}{(2\pi\sigma^2)^{1/4}} \exp\left(-\frac{t^2}{4\sigma^2}\right) \exp(i\omega_0 t), \quad (71)$$

such as in [1]. Here ω_0 is the mean frequency of the photon. One gets

$$\text{Re}\langle\psi_{+\delta}|\psi_{-\delta}\rangle = \cos(2\delta\omega_0) e^{-\frac{\delta^2}{2\sigma^2}}, \quad (122)$$

and hence the postselection probability becomes

$$p = \frac{1 - \cos(\omega_0\Delta\tau) e^{-\frac{\Delta\tau^2}{8\sigma^2}}}{2}. \quad (\text{Gaussian case}) \quad (123)$$

Note that the contribution of the cosine corresponds to a phase shift of the wave packets (originated by the time dilation) whereas the exponential contribution is the effect of the time dilation. This can be seen by looking at the Newtonian limit of the postselection probability, see eq (77), where the phase shift $\omega_0\Delta\tau$ can be explained by a gravitational Aharonov-Bohm effect:

$$p^{\text{NL}} = \frac{1 - \cos(\omega_0\Delta\tau)}{2}. \quad (124)$$

The direct detection of the gravitational time dilation via the postselection probability (123) is unpromising for two reasons. First it is very insensitive to small $\Delta\tau$ and second the cosine

(and therefore the phase shift) is the dominating contribution for small $\Delta\tau$. This can be seen by expanding (123) for small $\Delta\tau$:

$$p = \frac{1}{4} \left(\frac{1}{4\sigma^2} + \omega_0^2 \right) \Delta\tau^2 + \mathcal{O}(\Delta\tau^4) . \quad (125)$$

The condition (89) states that $1/4\sigma^2 < \omega_0^2$ and hence $\omega_0^2 \Delta\tau^2$ is the leading contribution in the post selection probability. This is originated by the cosine, thus the phase shift is the dominating effect and not the time dilation. Furthermore the lowest order is still quadratic in $\Delta\tau$.

Hence finding a pulse shape that is, to lowest order, linear in $\Delta\tau$ will increase the sensitivity of the postselection probability dramatically. Moreover the time dilation effect then predominates. Such a shape is trivially given by a rectangular pulse:

$$\psi(t) = \begin{cases} \frac{\exp(i\omega_0 t)}{(12\sigma^2)^{1/4}} & -\sqrt{3}\sigma \leq t \leq \sqrt{3}\sigma , \\ 0 & \text{otherwise} . \end{cases} \quad (126)$$

It is constructed such that $|\psi|^2$ is normalised to 1 and σ equals its standard deviation. The postselection probability for this pulse can easily calculated analytically using

$$\text{Re}\langle\psi_{+\delta}|\psi_{-\delta}\rangle = \begin{cases} \cos(2\delta\omega_0) \left(1 - \frac{\delta}{\sqrt{3}\sigma}\right) & \delta \leq \sqrt{3}\sigma , \\ 0 & \delta > \sqrt{3}\sigma , \end{cases} \quad (127)$$

so that one obtains

$$p = \frac{1}{2} \begin{cases} 1 - \cos(\omega_0 \Delta\tau) \left(1 - \frac{\Delta\tau}{2\sqrt{3}\sigma}\right) & \Delta\tau \leq 2\sqrt{3}\sigma , \\ 1 & \Delta\tau > 2\sqrt{3}\sigma . \end{cases} \quad (\text{rectangular case}) \quad (128)$$

For small $\Delta\tau$ this is linear in $\Delta\tau$:

$$p = \frac{1}{4\sqrt{3}} \frac{\Delta\tau}{\sigma} + \mathcal{O}(\Delta\tau^2) . \quad (129)$$

Moreover the drop in the postselection probability is clearly dominated by the time dilation of the wave packets in comparison to the phase shift $\omega_0 \Delta\tau$.

Figure 10 shows the postselection probability for a Gaussian pulse and for a rectangular pulse in dependence of the cross section of the interferometer for several frequencies and pulse widths.

But photons with a perfect rectangular pulse are nonphysical. Note that both the linearity in $\Delta\tau$ and the predominance of the time dilation effect base on the discontinuity of the rectangular pulse. This example just shows that the postselection probability depends on the shape of the photon⁶.

⁶Hence one could try to model the transition from rounded to sharp edges.

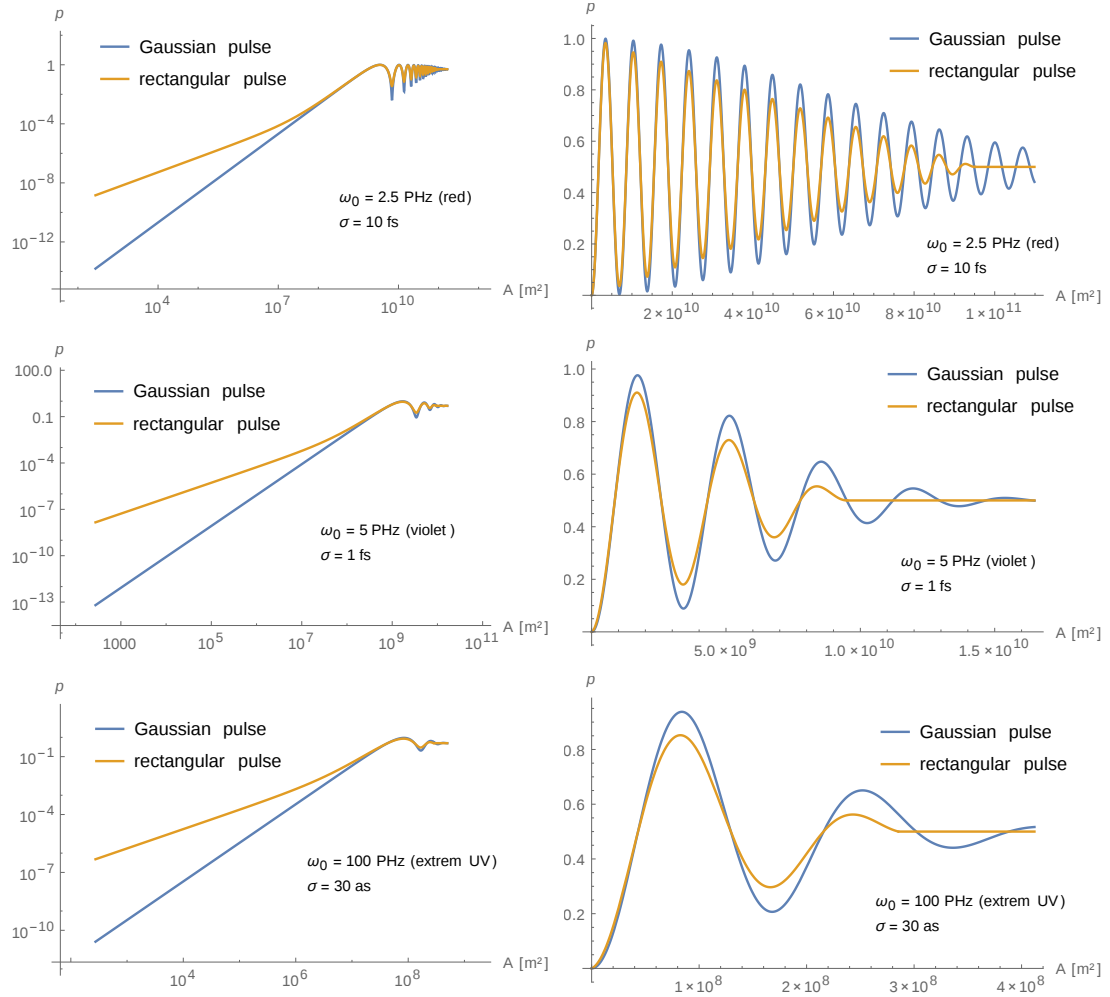


Figure 10: Postselection probability p for a photon to pass the second polariser P2 in dependence of the cross section $A = \frac{c^3}{g} \Delta\tau$ of the interferometer. The left graphs are log-log plots whereas the right graphs have linear axes.

However, also for a Gaussian shape the sensitivity of the postselection probability to $\Delta\tau$ can be made linear by introducing an additional controllable time delay ΔT . This additional time delay can be realised via nanopositioners or subnanopositioners which can change the arm length of one interferometer arm in the nanometer or subnanometer regime. In analogy to (123) the postselection probability then reads

$$p = \frac{1 - \cos(\omega_0(\Delta T + \Delta\tau)) e^{-\frac{(\Delta T + \Delta\tau)^2}{8\sigma^2}}}{2}. \quad (130)$$

If the additional time delay is chosen to be equal to one period of the photon,

$$\Delta T := \frac{2\pi}{\omega_0}, \quad (131)$$

the cosine part $\cos(\omega_0(\Delta T + \Delta\tau)) = \cos(\omega_0\Delta\tau)$ will only give quadratic contributions to the postselection probability whereas the exponential part is, to lowest order, linear in $\Delta\tau$. An expansion of (130) about $\Delta\tau = 0$ yields:

$$p = \frac{1 - e^{-\frac{\pi^2}{2\omega_0^2\sigma^2}}}{2} + \frac{\pi^2}{\omega_0^2\sigma^2} e^{-\frac{\pi^2}{2\omega_0^2\sigma^2}} \Delta\tau + \mathcal{O}(\Delta\tau^2). \quad (132)$$

For optical photons with $\omega_0 = 10^{15}$ Hz the additional time delay corresponds to an additional path length of $c\Delta T = 2\pi c/\omega_0 \approx 1.8 \mu\text{m}$. This is clearly in the feasible regime. The measurable quantity is now given by the change of the postselection probability when $\Delta\tau$ changes from zero to a positive value by placing the interferometer in the gravitational field. Since, for a given $\Delta\tau$ (rather for a given surface of the interferometer), the remaining free parameter is the pulse width σ , the change in the postselection probability can be maximised over σ :

$$\Delta p_{\max} := \max_{\sigma \geq 1/\omega_0} [p(\Delta\tau) - p(0)] = \max_{\sigma \geq 1/\omega_0} \left[\frac{1}{2} \left(e^{-\frac{\pi^2}{2\omega_0^2\sigma^2}} - \cos(\omega_0\Delta\tau) e^{-\frac{(2\pi/\omega_0 + \Delta\tau)^2}{8\sigma^2}} \right) \right]. \quad (133)$$

Here Δp_{\max} represents the maximal change of the postselection probability. The maximising pulse width, denoted by σ_{\max} , can be found analytically and reads:

$$\sigma_{\max} = \frac{1}{2\sqrt{2}} \sqrt{\frac{4\pi\Delta\tau/\omega_0 + \Delta\tau^2}{\ln \cos(\omega_0\Delta\tau) + 2 \ln \left(1 + \frac{\omega_0\Delta\tau}{2\pi} \right)}}. \quad (134)$$

Finally the maximal relative change κ_{\max} of the postselection probability is introduced by

$$\kappa_{\max} := \frac{\Delta p_{\max}}{p(\Delta\tau = 0, \sigma = \sigma_{\max})} = \frac{e^{-\frac{\pi^2}{2\omega_0^2\sigma_{\max}^2}} - \cos(\omega_0\Delta\tau) e^{-\frac{(2\pi/\omega_0 + \Delta\tau)^2}{8\sigma_{\max}^2}}}{1 - e^{-\frac{\pi^2}{2\omega_0^2\sigma_{\max}^2}}}. \quad (135)$$

In Fig. 11 solutions of this maximisation problem are shown for different mean frequencies. A lowest order approximation yields the following solutions of the maximisation problem:

$$\kappa_{\max} \approx \frac{1}{2\sqrt{2}} \frac{1}{e-1} \frac{\Delta\tau}{\sigma_{\max}}, \quad \Delta p_{\max} \approx \frac{1}{2e\sqrt{2}} \frac{\Delta\tau}{\sigma_{\max}}, \quad \sigma_{\max} \approx \frac{\pi}{\sqrt{2}} \frac{1}{\omega_0}, \quad \Delta T = \frac{2\pi}{\omega_0}. \quad (136)$$

In conclusion consider the following numerical example: A source emits 10^9 red photons ($\omega_0 = 2.5 \cdot 10^{15}$ Hz) per second. Assume that the photon detector is able to distinguish changes of the photon flux by 0.1%, thus $\kappa_{\max} = 10^{-3}$. The required additional time delay is given by $\Delta T = 2.51$ fs which corresponds to an additional path length of $c\Delta T = 0.75 \mu\text{m}$. The ideal pulse width reads $\sigma_{\max} = 0.89$ fs and the required cross section of the interferometer is $A = 11.9 \text{ km}^2$. Without gravity the postselection probability is $p = 31.5\%$ and changes to $(1 + \kappa_{\max})p$ in the gravitational case. Thus $3.15 \cdot 10^5$ additional photons per second arrive at the detector.

Compared to the original suggestion of 10^3 km^2 [1] this method represents an improvement of two orders of magnitude concerning the cross section of the interferometer. But still this is challenging with current technology.

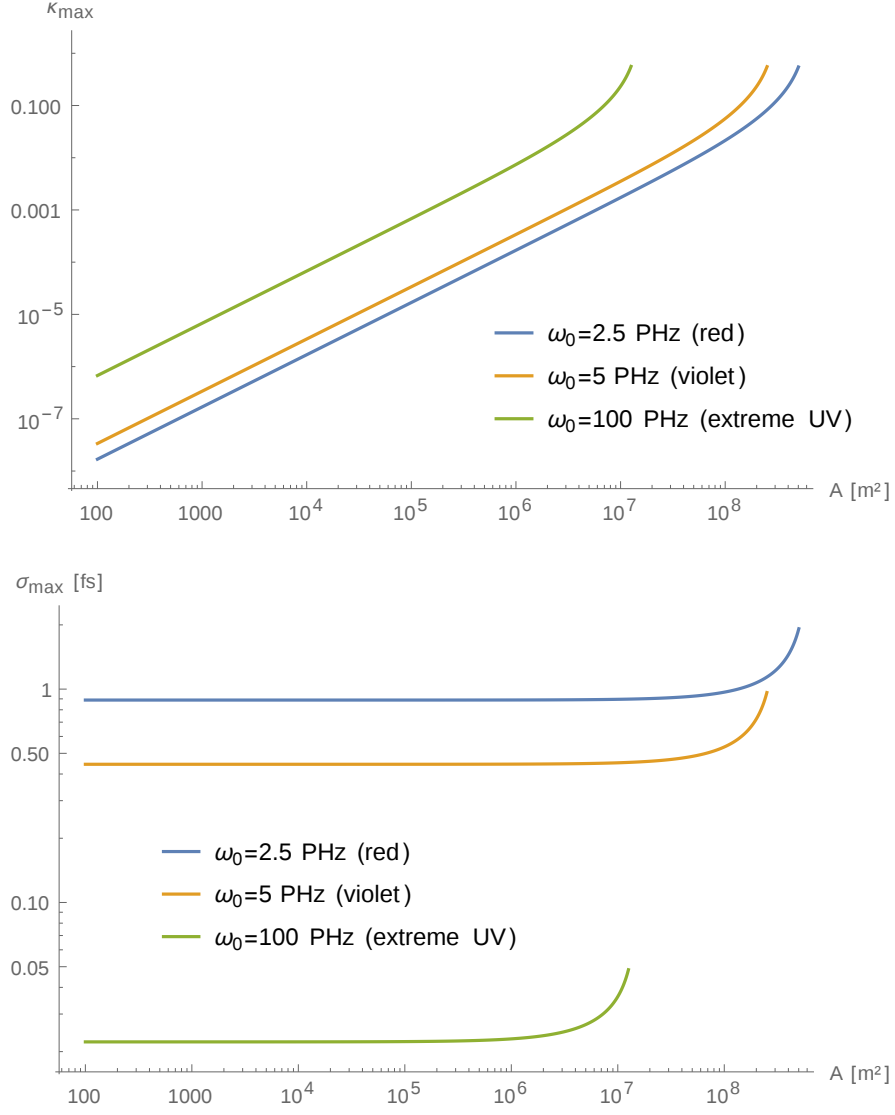


Figure 11: Solutions of the maximisation problem (133) in terms of the relative change κ_{max} of the postselection probability and σ_{max} for several frequencies in dependence of the cross section A of the interferometer.

5.4 Method 4: Shaping double-humped photons

In this method the attention is turned to the shape of the photons after the postselection. Here "shape" means the shape of the photon's wave function in the time domain. In the operational sense this shape is relevant to a time of arrival measurement. Under certain conditions the wave packet of the photon becomes a double-humped shape with two maxima and a dip between. This shape can be very sensitive to changes of the gravitational time dilation which manifests itself in a drop or a lift of the dip between the two maxima. However, it turns out that the same effect occurs in the Newtonian limit. Thus this method can not serve as a method to proof the gravitational time dilation but rather the gravitational phase shift.

The occurrence of a double-humped shape after postselections was already pointed out by Sudarshan and Stevenson [12]: If the postselection at the second polariser P2 produces a weak value (69) which is too large such that the conditions (72) and (73) are violated, the weak measurement formalism and its predictions are no longer applicable and a double-humped shape appears. This happens if the preselected polarisation is almost or even perfectly orthogonal to the postselected polarisation.

According to [12] the double-humped shape appears in its purest form if the preselected and postselected state are perfectly orthogonal and if the initial wave packet is real. Hence an orthogonal postselection is not sufficient to obtain a double-humped shape, if the initial wave packet has a complex phase. Note that Sudarshan and Stevenson [12] used a purely real Gaussian wave packet whereas here the wave packet, which represents the photon, has a complex phase. This complex phase is necessary in order to model a physical frequency distribution. For simplicity and in order to keep the analogy with [12] consider a photon with a Gaussian shape and a simple complex phase as given in eq. (71):

$$\psi(t) = \frac{1}{(2\pi\sigma^2)^{1/4}} \exp\left(-\frac{t^2}{4\sigma^2}\right) \exp(i\omega_0 t) , \quad (71)$$

The preselected polarisation $|I\rangle$ and the postselected polarisation $|F\rangle$ are chosen as orthogonal states,

$$|I\rangle = \frac{1}{\sqrt{2}}(|H\rangle + |V\rangle) , \quad (137)$$

$$|F\rangle = \frac{1}{\sqrt{2}}(|H\rangle - |V\rangle) . \quad (138)$$

which corresponds to $\alpha = -\beta = \pi/4$, $\chi = \varphi = 0$ such that the shape of the postselected photon reads (see eq. 63):

$$f(t) := |\psi_F(t)|^2 = \frac{1}{\sqrt{2\pi\sigma^2}} \frac{e^{-\frac{t^2}{2\sigma^2}} e^{-\frac{\Delta\tau^2}{8\sigma^2}} \left(\cosh\left(\frac{t\Delta\tau}{2\sigma^2}\right) - \cos(\omega_0\Delta\tau) \right)}{1 - \cos(\omega_0\Delta\tau) e^{-\frac{\Delta\tau^2}{8\sigma^2}}} . \quad (139)$$

For a simpler notation this photon shape is henceforth denoted by $f(t)$. By putting $\omega_0 = 0$ the cosine in the numerator becomes 1 and therefore f clearly represents a double-humped

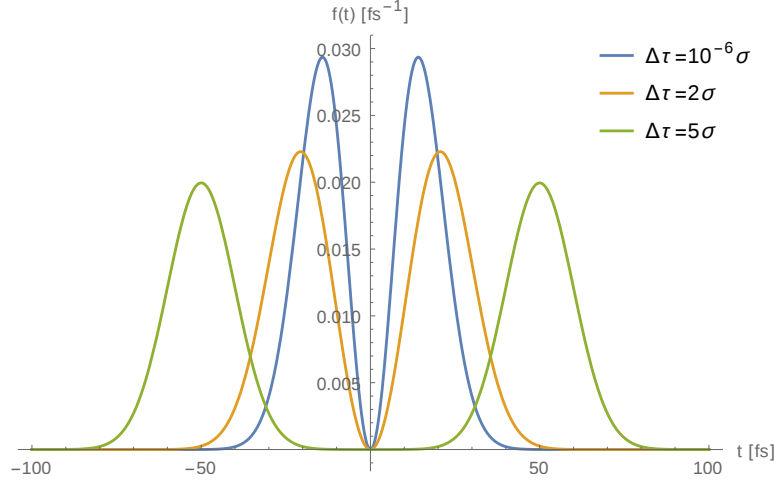


Figure 12: Plot of $f(t)$ for $\omega_0 = 0$ such that the Gaussian wave function $\psi(t)$ is purely real as given by (71). The pulse width is chosen as $\sigma = 10$ fs. One can see that the two maxima are approximately located at $\pm\sqrt{2}\sigma$ for $\Delta\tau \ll \sigma$ and at $\pm\Delta\tau$ for $\Delta\tau \gg \sigma$.

function corresponding to the case in [12]. This can be seen by keeping in mind that $f \geq 0$ decays for $t \rightarrow \pm\infty$ whereas $f(t=0) = 0$. Figure 12 shows $f(t)$ for $\omega_0 = 0$, $\sigma = 10$ fs, and several $\Delta\tau$. But for $\omega_0 > 0$ this argument does not hold in general, since the cosine in the numerator is no longer equal to 1.

In order to find the conditions to restore the double-humped shape of f for $\omega_0 > 0$ one can look at the second derivative of f at $t = 0$ which necessarily has to be greater than zero to obtain a minimum of f at $t = 0$. The fact that f has an extremum at $t = 0$ is granted by

$$\frac{\partial}{\partial t}f|_{t=0} = 0. \quad (140)$$

Since the second derivative of f at $t = 0$ is given by

$$\frac{\partial^2}{\partial t^2}f|_{t=0} = \sqrt{\frac{2}{\pi}} \frac{1}{\sigma^3} \frac{e^{-\frac{\Delta\tau^2}{8\sigma^2}}}{1 - \cos(\omega_0\Delta\tau)e^{-\frac{\Delta\tau^2}{8\sigma^2}}} \left(\frac{\Delta\tau^2}{8\sigma^2} - \sin^2\left(\frac{\omega_0\Delta\tau}{2}\right) \right), \quad (141)$$

one can define the auxiliary function $q(t)$ by neglecting the positive part of (141):

$$q(t) := \frac{t^2}{8\sigma^2} - \sin^2\left(\frac{\omega_0 t}{2}\right). \quad (142)$$

The necessary condition for a double humped shape of f then reads: $q(\Delta\tau) > 0$. One can clearly see that $q(\Delta\tau, \omega_0 = 0) = \Delta\tau^2/8\sigma^2 > 0$ is always fulfilled but for $\omega_0 > 0$ the condition $q(\Delta\tau) > 0$ constitutes a non-trivial relation between σ , ω_0 , and $\Delta\tau$. Expanding

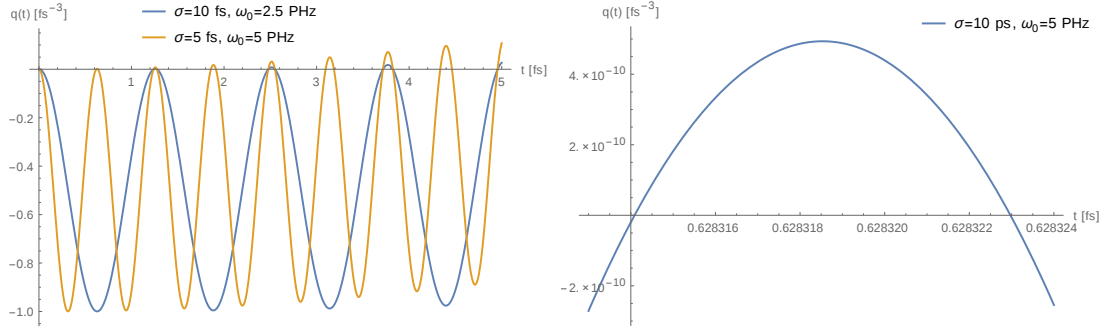


Figure 13: Plots of $q(t)$ for different pulse widths σ and mean frequencies ω_0 . The left graph illustrates how changes of σ and ω_0 affect the graph of q . The right plot shows the first positive maximum of q for $\sigma = 10^{-11}$ s and $\omega_0 = 5 \cdot 10^{15}$ Hz. This illustrates the narrowness of the positive areas of q .

$q(\Delta\tau)$ for small $\Delta\tau$ yields

$$q(\Delta\tau) = \frac{\Delta\tau^2}{8\sigma^2} - \frac{\omega_0^2 \Delta\tau^2}{4} + \mathcal{O}(\Delta\tau^4), \quad (143)$$

such that the condition $q(\Delta\tau) > 0$ is equivalent to $\sigma\omega_0 < 1/\sqrt{2}$. But this violates the condition (89) for producible photons. Thus for $\Delta\tau$ in the sub-pulse-width regime no double-humped photons occur behind the second polariser P2. Figure 13 shows plots of $q(t)$ for different choices of σ and ω_0 : The intervals of positive q are very narrow for an appropriate choice of σ and ω_0 . Since the double-humped shape occurs only for time dilations within these intervals the following strategy is advisable:

An additional controllable time delay ΔT is introduced such that a variation of the gravitational time dilation $\Delta\tau$ (rotating the interferometer in the gravitational field) happens inside the interval where q is positive. The additional time delay ΔT can be controlled by positioner elements to vary the arm length of the interferometer. If these intervals of positive q are sufficiently narrow⁷ a variation of the gravitational time dilation could have a measurable effect of the double-humped shape: the dip between the two humps of f is dropped or lifted (see Fig. 15). A measurable effect is expected if the length of the intervals of positive q is only one or two orders of magnitude larger than the gravitational time dilation.

According to this strategy it is useful to find the length of the intervals of positive q , see Fig. 14. Even though it is not possible to find an analytical exact expression, the following

⁷Note that the shape of the photon experiences a drastic change (single-humped \rightarrow double-humped \rightarrow single-humped) if the time dilation is varied from one end of the interval of positive q to the other. In practice the variation can hardly be made so large. However the variation of the gravitational time dilation needs to be of an amount comparable to the length of the interval of positive q .

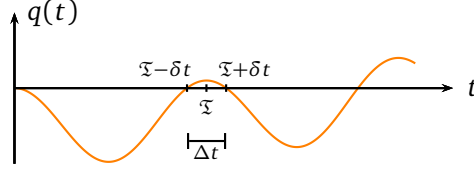


Figure 14: Sketch of q to illustrate the first positive area. The position of the first maximum is denoted by \mathfrak{T} and δt is approximately the distance to the closest zeros. The length of the interval where q is positive is denoted by $\Delta t \approx 2\delta t$.

approximation can be considered: Expand q in the area of its first positive maximum up to quadratic order for given σ and ω_0 . The intersections with the abscissa then reveal the length of these intervals of positive q .

Let \mathfrak{T} be the point of the first positive maximum of q for given σ and ω_0 :

$$\mathfrak{T} := \min \left\{ t \mid t > 0, q(t) > 0, q'(t) = 0, q''(t) < 0 \right\}. \quad (144)$$

Now expand $q(\mathfrak{T} + \delta t)$ for small deviations δt :

$$\begin{aligned} q(\mathfrak{T} + \delta t) &= q(\mathfrak{T}) + \overbrace{q'(\mathfrak{T})\delta t}^{0 \text{ by def.}} + \frac{1}{2}q''(\mathfrak{T})\delta t^2 + \mathcal{O}(\delta t^3) \\ &= \frac{\mathfrak{T}^2}{8\sigma^2} - \sin^2\left(\frac{\omega_0\mathfrak{T}}{2}\right) + \frac{1}{2}\left(\frac{1}{4\sigma^2} - \frac{\omega_0^2}{2}\cos(\omega_0\mathfrak{T})\right)\delta t^2 + \mathcal{O}(\delta t^3) \\ &= \frac{\mathfrak{T}^2}{8\sigma^2} - \frac{1}{2} + \frac{1}{2}\sqrt{1 - \frac{\mathfrak{T}^2}{4\sigma^4\omega_0^2}} + \frac{1}{4}\left(\frac{1}{2\sigma^2} - \omega_0^2\sqrt{1 - \frac{\mathfrak{T}^2}{4\sigma^4\omega_0^2}}\right)\delta t^2 + \mathcal{O}(\delta t^3). \end{aligned} \quad (145)$$

Here the fact that $q'(\mathfrak{T}) = 0$ was used, which is equivalent to

$$\sin(\omega_0\mathfrak{T}) = \frac{\mathfrak{T}}{2\sigma^2\omega_0}, \quad (146)$$

hence one made use of

$$\cos(\omega_0\mathfrak{T}) = \sqrt{1 - \sin^2(\omega_0\mathfrak{T})} = \sqrt{1 - \frac{\mathfrak{T}^2}{4\sigma^4\omega_0^2}}, \quad (147)$$

and

$$\sin^2\left(\frac{\omega_0\mathfrak{T}}{2}\right) = -\frac{1}{2} + \frac{1}{2}\cos(\omega_0\mathfrak{T}) = -\frac{1}{2} + \frac{1}{2}\sqrt{1 - \frac{\mathfrak{T}^2}{4\sigma^4\omega_0^2}}. \quad (148)$$

To find the roots of q one can now solve $q(\mathfrak{T} + \delta t) = 0$ for δt by neglecting the $\mathcal{O}(\delta t^3)$ terms. The solution is given by:

$$\delta t \approx 2 \sqrt{\frac{\frac{\mathfrak{T}^2}{4\sigma^2} - 1 + \sqrt{1 - \frac{\mathfrak{T}^2}{4\sigma^4\omega_0^2}}}{2\omega_0^2\sqrt{1 - \frac{\mathfrak{T}^2}{4\sigma^4\omega_0^2}} - \frac{1}{\sigma^2}}}. \quad (149)$$

But since \mathfrak{T} is unknown this expression is not helpful yet. Even though \mathfrak{T} will remain unknown in general one can specify the exact solution in the limit $\sigma\omega_0 \rightarrow \infty$. In this limit where the product of σ and ω_0 goes to infinity the points of positive maxima of q are given by $\mathfrak{T}_n = \frac{2\pi n}{\omega_0}$, $n \in \mathbb{N}^+$. This can be proven in the following way:

$$q(\mathfrak{T}_n) = \frac{\pi^2 n^2}{2\sigma^2} - \sin^2(\pi n) = \frac{\pi^2 n^2}{2\sigma^2} > 0, \quad (150)$$

$$q'(\mathfrak{T}_n) = \frac{\pi n}{2\sigma^2 \omega_0} - \frac{\omega_0}{2} \sin(2\pi n) = \frac{\pi}{2\sigma} \frac{1}{\sigma \omega_0} \xrightarrow{\sigma \omega_0 \rightarrow \infty} 0, \quad (151)$$

$$q''(\mathfrak{T}_n) = \frac{1}{4\sigma^2} - \frac{\omega_0^2}{2} \cos(2\pi n) = \frac{\omega_0^2}{2} \left(\frac{1}{2\sigma^2 \omega_0^2} - 1 \right) \xrightarrow{\sigma \omega_0 \rightarrow \infty} -\frac{\omega_0^2}{2} < 0. \quad (152)$$

Thus, in the limit $\sigma\omega_0 \rightarrow \infty$, the point of the first positive maximum of q is given by $\mathfrak{T}_1 = \frac{2\pi}{\omega_0}$. Indeed, producible photon pulses are far from the limit $\sigma\omega_0 \rightarrow \infty$, but for $\sigma\omega_0 \gg 1$ one can still assume⁸ that \mathfrak{T} is of the order of $\frac{2\pi}{\omega_0}$.

In order to turn (149) into a useful expression, substitute $X = \frac{\omega_0}{2\pi} \mathfrak{T}$ and $\varepsilon = \frac{1}{\sigma\omega_0}$. Now X is a quantity of the order of 1 whereas ε is small if $\sigma\omega_0 \gg 1$. This yields

$$\delta t \approx \frac{2}{\omega_0} \sqrt{\frac{X^2 \pi^2 \varepsilon^2 - 1 + \sqrt{1 - X^2 \pi^2 \varepsilon^4}}{2\sqrt{1 - X^2 \pi^2 \varepsilon^4} - \varepsilon^2}}, \quad (153)$$

which can be expanded for small ε to get:

$$\delta t \approx \frac{\sqrt{2}X\pi}{\omega_0} \varepsilon + \mathcal{O}(\varepsilon^5) \approx \frac{\sqrt{2}\pi}{\sigma\omega_0} \frac{1}{\omega_0}, \quad (154)$$

Using this approximation one arrives at the solution of the length Δt of the first interval where q is positive, which is just given by $\Delta t \approx 2\delta t$:

$$\Delta t \approx \frac{2\sqrt{2}\pi}{\sigma\omega_0} \frac{1}{\omega_0}. \quad (155)$$

So the double-humped shape of f occurs only if the time dilation remains in the small interval of positive q which has the length of Δt . To achieve these intervals an additional controllable time delay ΔT is necessary. One can define ΔT as the point where q becomes positive, see Fig. 14:

$$\Delta T : \approx \mathfrak{T} - \delta t \approx \frac{2\pi}{\omega_0} \left(1 - \frac{\sqrt{2}}{\sigma\omega_0} \right). \quad (156)$$

⁸A simple calculation shows that the smallest correction terms are negligible in the case of $\sigma\omega_0 \gg 1$.

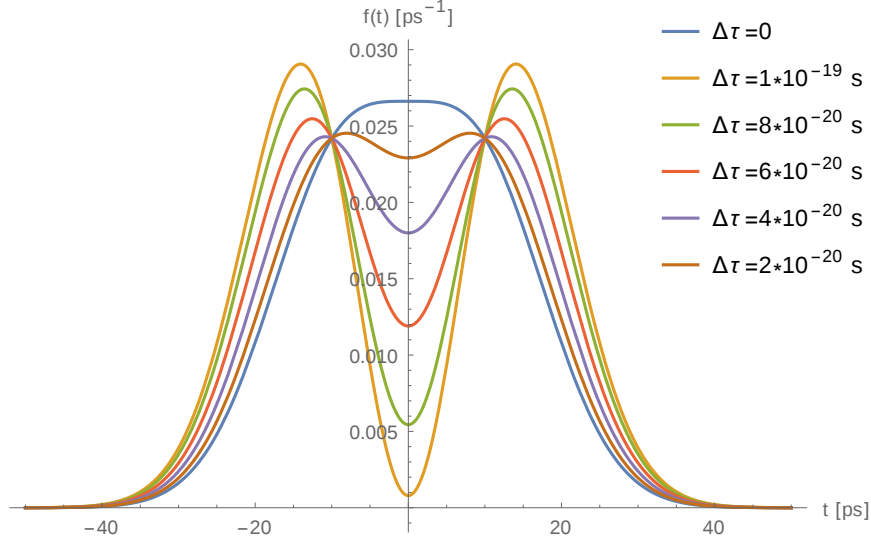


Figure 15: Plot of $f(t)$ where $\sigma = 10$ ps and $\omega_0 = 2 \cdot 10^{15}$ Hz for several gravitational time dilations $\Delta\tau$. The overall time dilation is given by $\Delta T + \Delta\tau$ where the controllable time dilation is $\Delta T = 3.14137 \cdot 10^{-15}$ s. A time of arrival measurement would detect two distinct arrival times which differ by an amount of ~ 30 ps (separation of the two humps) for $\Delta\tau \sim 10^{-20}$ s whereas this effect does not occur for $\Delta\tau = 0$.

Thus, for a time delay of ΔT , the shape of the photons are almost double-humped if there is no further gravitational time dilation ($\Delta\tau = 0$). In the case of a nonvanishing gravitational time dilation ($\Delta\tau > 0$), where the overall time dilation is given by $\Delta T + \Delta\tau$, the photon shape starts to become double-humped as long as $\Delta\tau < \Delta t$. In Fig. 15 an illustration of this effect is shown. Table 1 presents numerical solutions of Δt and ΔT for given σ and ω_0 which are in agreement with the approximations derived above.

Another important question is the separation of the two humps if f is double-humped. This separation corresponds to the difference of the arrival time of the photons to be measured. To find this separation one can set $\Delta T = \frac{2\pi}{\omega_0}$ in order to annihilate the cosine term in the numerator of f and to restore the double-humped shape. Besides normalisation, f reduces then to (see eq. 139)

$$f(t) \sim e^{-\frac{t^2}{2\sigma^2}} \left(\cosh\left(\frac{t\pi}{\sigma^2\omega_0}\right) - 1 \right). \quad (157)$$

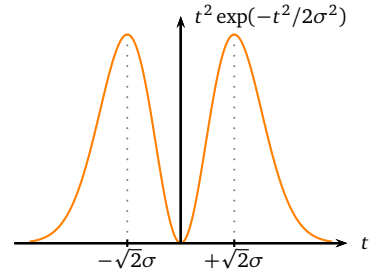


Figure 16: Sketch of $t^2 e^{(-t^2/2\sigma^2)}$

σ [ps]	ω_0 [PHz]	ΔT [fs]	Δt [zs]	A [10^4 m^2]
100	5	1.256635	3.5	0.98
10	4	1.57077	55.5	1.53
20	2	3.1415	111	3.05
10	2	3.1415	222	6.10
0.1	5	1.255	3554	97.6

Table 1: Numerical solutions of Δt and ΔT for given σ and ω_0 . Moreover $A = \frac{c^3 \Delta \tau}{g}$ is the area of an interferometer which corresponds to a gravitational time dilation of $\Delta \tau = 0.1 \Delta t$.

Keeping the assumption that the product $\sigma \omega_0$ is large an expansion of f reveals the double humped shape:

$$f(t) \sim t^2 e^{-\frac{t^2}{2\sigma^2}} \frac{1}{\sigma^2 \omega_0^2} + t^4 e^{-\frac{t^2}{2\sigma^2}} \cdot \mathcal{O}\left(\frac{1}{\sigma^4 \omega_0^4}\right). \quad (158)$$

Neglecting the terms of higher orders implies that the two humps are approximately located where $t^2 \exp(-t^2/2\sigma^2)$ is maximal. These maxima can easily be found via the first and second derivative and are located at $\pm\sqrt{2}\sigma$, see Fig. 16.

The two humps of f are approximately separated by $2\sqrt{2}\sigma$ if $\sigma \omega_0 \gg 1$.

In Fig. 15 the pulse width was chose as $\sigma = 10$ ps so that the two humps are approximately separated by $2\sqrt{2}\sigma = 28.28$ ps. This is feasible with current technology since available single-photon detectors have a resolution of 10 ps [17].

Finally the postselection probability p is calculated. The formula is already given by eq. (123) on p. 35. Again one sets $\Delta T = \frac{2\pi}{\omega_0}$ to achieve the double-humped shape of f . Hence one arrives at

$$p = \frac{1 - e^{-\frac{\pi^2}{2\sigma^2 \omega_0^2}}}{2} = \frac{\pi^2}{4\sigma^2 \omega_0^2} + \mathcal{O}\left(\frac{1}{\sigma^4 \omega_0^4}\right). \quad (159)$$

So to lowest order the postselection probability is given by

$$p \approx \frac{\pi^2}{4\sigma^2 \omega_0^2}. \quad (160)$$

This uncovers a major disadvantage of this method: for all practical purposes the postselection probability is extremely small. Consider, e.g., the values used in the example from Fig. 15. With these values the postselection probability becomes $6.2 \cdot 10^{-9}$. In the next subsection it is calculated to what extent the postselection probability can be increased by deviations from perfectly orthogonal postselections.

One may wonder why only the case $\sigma\omega_0 \gg 1$ is considered here? Although the postselection probability might be considerable, even if $\sigma\omega_0 \sim 1$, the length Δt of the interval of positive q becomes too large. If this interval is too large compared to the gravitational time dilation $\Delta\tau$, the shape of the photon will not change. See, e.g., Tab. 1: The smaller the product $\sigma\omega_0$ the larger is the required gravitational time dilation (the larger is the required surface of the interferometer). Furthermore large p and small Δt can not be achieved simultaneously. This can be seen by expressing p in terms of Δt (see eq. 160 and 155):

$$p \approx \frac{\omega_0^2}{32} \Delta t^2. \quad (161)$$

Thus, since ω_0 is bounded to optical frequencies, a sufficiently small Δt results in a very small postselection probability p .

Moreover, it clear, that the described effect is a phase shift effect and would therefore also occur in the Newtonian limit. The reason is that the occurrence of the double humped shape of f exclusively depends on the behaviour of the cosine in the numerator of (139). Thus it depends only on the phase shift $\omega_0\Delta\tau$ which is caused by the time dilation but could be also caused by a pure Aharonov-Bohm phase shift.

Another serious drawback of this method lies in the fact, that the accuracy of the additional controllable time dilation ΔT needs to be sufficiently high to find the region where q becomes positive and f becomes double-humped. So if the accuracy of ΔT is several orders of magnitude weaker than of Δt the double-humped regions are not achievable. Currently available nanopositioners have a resolution of $0.05 \text{ nm} = 50 \text{ pm}$ which corresponds to a resolution of 0.17 as for the controllable time delay. But if picopositioners with a resolution of 1 pm are available, the resolution of the additional controllable time dilation would be of the order of 3.34 zs . Thus gravitational phase shifts caused by time dilations in the subzeptosecond regime (which corresponds to a interferometer's surface of 10^3 m^2) would be accessible via the method presented here. Compared to a surface of 10^3 km^2 as calculated in [1] this would be an improvement of six orders of magnitude.

Increasing the postselection probability by deviations from orthogonal postselections

To model deviations from a orthogonal postselection the angle ε is introduced such that the postselection is no longer given by (138) but by

$$|F\rangle = \cos\left(-\frac{\pi}{4} + \varepsilon\right) |H\rangle + \sin\left(-\frac{\pi}{4} + \varepsilon\right) |V\rangle, \quad (162)$$

such that $|F\rangle = (|H\rangle - |V\rangle)/\sqrt{2}$ for $\varepsilon = 0$. Now f is no longer given by (139) but by

$$f(t) = \frac{\cos^2\left(-\frac{\pi}{4} + \varepsilon\right) |\psi(t + \delta)|^2 + \sin^2\left(-\frac{\pi}{4} + \varepsilon\right) |\psi(t - \delta)|^2 - \cos(2\varepsilon) \text{Re} \left[\overline{\psi(t + \delta)} \psi(t - \delta) \right]}{1 - \cos(2\varepsilon) \text{Re} \langle \psi_{-\delta}, \psi_{\delta} \rangle}. \quad (163)$$

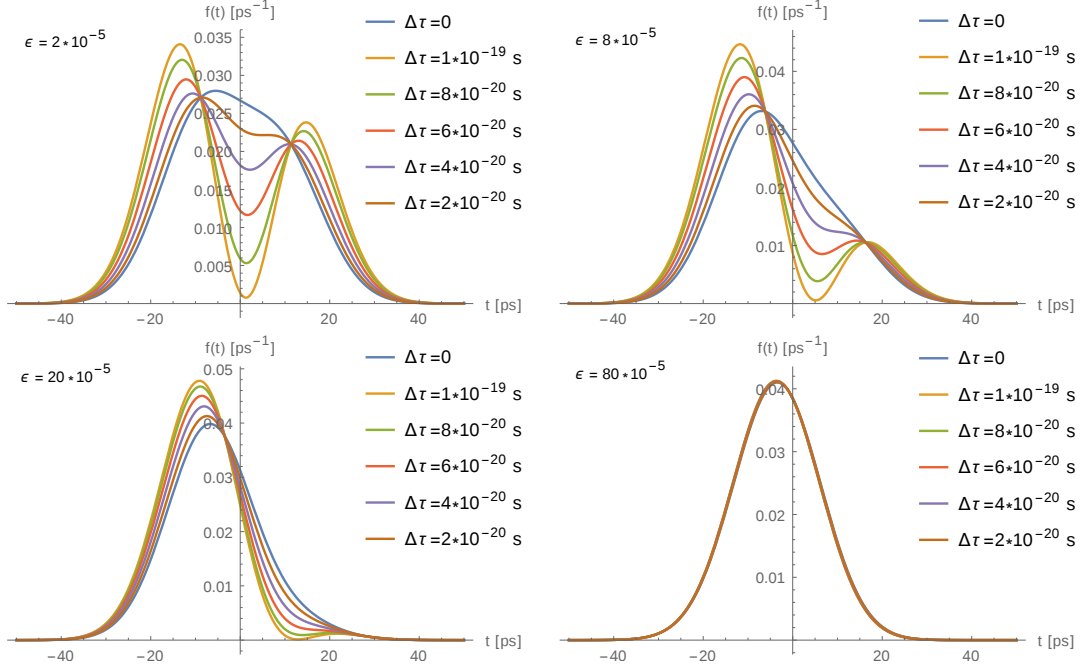


Figure 17: All four plots are recalculations of the example from Fig. 15 with exactly the same numerical values but for several $\varepsilon > 0$. One can clearly see, that the larger ε the more the shape is shifted towards the left hump. This indicates that the weak measurement formalism becomes valid. Note, that the weak measurements predict only a shift of the wave function.

Note that this is equal to (139) for $\varepsilon = 0$. Furthermore, in this subsection we do not consider $\psi(t)$ to be a Gaussian function but an arbitrary single-humped photon wave function with a simple phase: $\psi(t) = |\psi(t)| \exp(i\omega_0 t)$. The only assumptions are: $|\psi(t)|$ is centred and symmetric around $t = 0$ (e.g. Gaussian distribution, Lorentz distribution, sech distribution, etc.). Remember that $\delta = \frac{\Delta\tau}{2}$.

The postselection probability now reads:

$$p = \frac{1 - \cos(2\varepsilon) \text{Re} \langle \psi_{-\delta}, \psi_{\delta} \rangle}{2}. \quad (164)$$

Again, for $\varepsilon = 0$ this is equivalent to the case of a perfectly orthogonal postselection as discussed above. But for $|\varepsilon| > 0$ the $\cos(2\varepsilon)$ term increases the postselection probability. But also the double-humped shape of f decays into a single-humped shape if $|\varepsilon|$ becomes too large. Thus it is necessary to find a compromise between the increase of the postselection probability and the decay of the double humped shape. Figure 17 illustrates the decay of the double-humped shape of f for $|\varepsilon| > 0$: One hump grows whereas the other decays whereupon a single-humped shape appears.

To find this compromise one needs to define the region of ε where the double-humped shape of f is still present. Interestingly, the expectation value of f serves as a good measure

for its presence. This can be seen as follows: For $\varepsilon = 0$ the expectation value of f is located at $t = 0$ since both humps are equal. If ε is increased (decreased) the left (right) hump grows whereas the other shrinks. Thus the expectation value is pulled to the left (right). If ε is sufficiently large the dominant hump moves back to the origin at $t = 0$. Thus the dominant hump drags the expectation value back to the origin. Hence the maximal displacement of the expectation value of f due to growing $|\varepsilon|$ can serve as an indicator where the double-humped shape of f loses its presence.

Henceforth the expectation value of $f =: f_\varepsilon$ is denoted by $\mu(\varepsilon)$:

$$\mu(\varepsilon) := \int_{-\infty}^{+\infty} t f_\varepsilon(t) dt. \quad (165)$$

Since $|\psi|$ was assumed to be symmetric around $t = 0$ in the definition (163) of f , the expectation value $\mu(\varepsilon)$ can directly be calculated:

$$\mu(\varepsilon) = -\frac{\sin(2\varepsilon)}{1 - \cos(2\varepsilon)\text{Re}\langle\psi_{-\delta}, \psi_\delta\rangle} \delta. \quad (166)$$

The following was used to find $\mu(\varepsilon)$:

$$-\cos^2\left(-\frac{\pi}{4} + \varepsilon\right) + \sin^2\left(-\frac{\pi}{4} + \varepsilon\right) = -\sin(2\varepsilon), \quad (167)$$

$$\int_{-\infty}^{+\infty} t |\psi(t \pm \delta)|^2 dt = \int_{-\infty}^{+\infty} (t \mp \delta) |\psi(t)|^2 dt = \mp \delta, \quad (168)$$

and

$$\int_{-\infty}^{+\infty} t \text{Re} \left[\overline{\psi(t + \delta)} \psi(t - \delta) \right] dt = 0, \quad (169)$$

since the integrand is an odd function of t . In order to find the maximum of μ consider the first derivative:

$$\mu'(\varepsilon) = -2 \frac{\cos(2\varepsilon) - \text{Re}\langle\psi_{-\delta}, \psi_\delta\rangle}{(1 - \cos(2\varepsilon)\text{Re}\langle\psi_{-\delta}, \psi_\delta\rangle)^2} \delta \quad (170)$$

Hence $\mu'(\varepsilon) = 0$ is trivially solved by

$$\begin{aligned} \varepsilon_{\text{trans}} &= \frac{1}{2} \arccos(\text{Re}\langle\psi_{-\delta}, \psi_\delta\rangle) \\ &= \frac{1}{2} \arccos\left(\cos(\omega_0 \Delta \tau) \int_{-\infty}^{\infty} \left| \psi\left(t + \frac{\Delta \tau}{2}\right) \right| \left| \psi\left(t - \frac{\Delta \tau}{2}\right) \right| dt\right), \end{aligned} \quad (171)$$

where the assumption $\psi(t) = |\psi(t)|e^{i\omega_0 t}$ was used. That this is a maximum can be seen by checking $\mu''(\varepsilon_{\text{trans}}) < 0$. The region of allowed deviations from an orthogonal postselection is given by

$$\varepsilon \in [-\varepsilon_{\text{trans}}, +\varepsilon_{\text{trans}}]. \quad (172)$$

This result allows to calculate the maximal postselection probability by applying the maximal allowed deviation from the orthogonal postselection: Set $\varepsilon = \pm \varepsilon_{\text{trans}}$ to obtain

$$p_{\text{max}} = \frac{1 - \cos(\pm 2\varepsilon_{\text{trans}}) \text{Re}\langle \psi_{-\delta}, \psi_{\delta} \rangle}{2} = \frac{1 - (\text{Re}\langle \psi_{-\delta}, \psi_{\delta} \rangle)^2}{2}. \quad (173)$$

Using the assumption $\psi(t) = |\psi(t)|e^{i\omega_0 t}$ one can write:

$$p_{\text{max}} = \frac{1 - \cos^2(\omega_0 \Delta \tau) \left(\int_{-\infty}^{\infty} |\psi(t + \frac{\Delta \tau}{2})| |\psi(t - \frac{\Delta \tau}{2})| dt \right)^2}{2}. \quad (174)$$

Now one can again consider the case where the double-humped shape of f occurs, so one sets $\Delta T = \frac{2\pi}{\omega_0}$. For a Gaussian ψ this results in

$$p_{\text{max}} = \frac{1 - e^{-\frac{\pi^2}{\sigma^2 \omega_0^2}}}{2} = \frac{\pi^2}{2\sigma^2 \omega_0^2} + \mathcal{O}\left(\frac{1}{\sigma^4 \omega_0^4}\right). \quad (\text{Gaussian case}) \quad (175)$$

Thus to lowest order the maximal postselection probability is given by

$$p_{\text{max}} \approx \frac{\pi^2}{2\sigma^2 \omega_0^2}. \quad (\text{Gaussian case}) \quad (176)$$

Comparing this result with the non-maximised postselection probability (160) is rather disappointing: p_{max} is only twice as large as in the case of an orthogonal postselection. Thus, by deviating from perfectly orthogonal postselections the postselection probability can only be doubled.

With different initial pulse shapes one can gain little enhancement of the postselection probability, however, the resulting postselection probabilities will remain of the same order of magnitude. Consider, for example, a hyperbolic secant distribution (sech):

$$\psi(t) = \sqrt{\frac{\pi}{4\sqrt{3}\sigma}} \text{sech}\left(\frac{\pi}{2\sqrt{3}\sigma} t\right) e^{i\omega_0 t}, \quad (177)$$

where

$$\text{sech } t = \frac{1}{\cosh t} = \frac{2}{e^t + e^{-t}}. \quad (178)$$

Here σ appears such that it is equal to the standard deviation of $|\psi|^2$ as before. A calculation offers:

$$p_{\text{max}} = \frac{1 - \frac{4\pi^4}{3\sigma^2 \omega_0^2} \text{csch}^2\left(\frac{2\pi^2}{\sqrt{3}\sigma \omega_0}\right)}{2} = \frac{2\pi^4}{9\sigma^2 \omega_0^2} + \mathcal{O}\left(\frac{1}{\sigma^4 \omega_0^4}\right), \quad (\text{Sech case}) \quad (179)$$

where

$$\text{csch } t = \frac{1}{\sinh t} = \frac{2}{e^t - e^{-t}}. \quad (180)$$

Thus to lowest order one gets

$$p_{\max} \approx \frac{2\pi^4}{9\sigma^2\omega_0^2}, \quad (\text{Sech case}) \quad (181)$$

which is larger by a factor of $4\pi^2/9 \approx 4.39$ compared to the Gaussian case.

5.5 Method 5: Cutting out frequencies

Instead of measuring the shape of the photon the frequency distribution of the postselected photons is of interest in this method. Under certain conditions the interference at the second polarising beam splitter PBS2 in combination with the postselection at P2 cuts out a certain frequency. The gravitational phase shift caused by the gravitational time dilation can shift these cut out frequency in a measurable way. A measurement can be conducted with a gas which absorbs photons with a certain frequency. If this frequency is cut out the photons pass the gas whereas they will be absorbed by the gas if the cut out frequency is shifted due to the gravitational phase.

The effect of a cut out frequency can be seen by looking at the state after the postselection where the following preselection and postselection was chosen:

$$|I\rangle = \frac{1}{\sqrt{2}}(|H\rangle + |V\rangle) , \quad (182)$$

$$|F\rangle = \frac{1}{\sqrt{2}}(|H\rangle + e^{i\varphi}|V\rangle) . \quad (183)$$

This results in the final state (see eq. 63):

$$\psi_F(t) = \frac{\psi(t+d+\delta) + e^{-i\varphi}\psi(t-d-\delta)}{\sqrt{2(1 + \cos\varphi \operatorname{Re}\langle\psi_{-d-\delta}, \psi_{+d+\delta}\rangle)}} , \quad (184)$$

where an additional controllable time delay $\Delta T \equiv 2d$ (via positioner elements) was introduced on top of the gravitational time dilation $\Delta\tau \equiv 2\delta$. In the frequency basis the state reads

$$\tilde{\psi}_F(\omega) = \sqrt{\frac{2}{1 + \cos\varphi \operatorname{Re}\langle\psi_{-d-\delta}, \psi_{+d+\delta}\rangle}} \tilde{\psi}(\omega) \cos\left(\omega(d+\delta) + \frac{\varphi}{2}\right) . \quad (185)$$

Here the tilded functions correspond to the Fourier transformations:

$$\tilde{\psi}(\omega) = \frac{1}{\sqrt{2\pi}} \int \psi(t) e^{-i\omega t} dt . \quad (186)$$

Hence after the postselection the frequency distribution of the photon is given by $|\tilde{\psi}_F|^2$ which will be denoted by \tilde{f} :

$$\tilde{f}(\omega) := |\tilde{\psi}_F(\omega)|^2 = \frac{2}{1 + \cos\varphi \operatorname{Re}\langle\psi_{-d-\delta}, \psi_{+d+\delta}\rangle} |\tilde{\psi}(\omega)|^2 \cos^2\left(\omega(d+\delta) + \frac{\varphi}{2}\right) . \quad (187)$$

It is assumed that $|\tilde{\psi}(\omega)|^2$ (frequency distribution before the postselection) is single-peaked at $\omega = \omega_0$. However, in the frequency distribution $\tilde{f}(\omega)$ after the postselection, $|\tilde{\psi}(\omega)|^2$ is multiplied by \cos^2 which is zero at

$$\omega = \frac{\pi\left(n + \frac{1}{2}\right) - \frac{\varphi}{2}}{d + \delta} , \quad n \in \mathbb{N} . \quad (188)$$

Thus, for given ω_0 , one can choose the controllable time delay as

$$d := \frac{\pi \left(n + \frac{1}{2}\right) - \frac{\varphi}{2}}{\omega_0}, \quad \text{for some fix } n \in \mathbb{N}. \quad (189)$$

For this choice of d the frequency distribution $\tilde{f}(\omega)$ is 0 at $\omega = \omega_0$ in the absence of a gravitational time dilation ($\delta = \Delta\tau/2 = 0$) since the \cos^2 is 0 at $\omega = \omega_0$. Hence, for this choice of d , \tilde{f} gets a double-humped shape where the frequency ω_0 is cut out.

To see this double-humped shape in an analytical form, consider the case where $\tilde{\psi}(\omega)$ is Gaussian,

$$\tilde{\psi}(\omega) = \frac{1}{(2\pi\tilde{\sigma}^2)^{1/4}} e^{-\frac{(\omega-\omega_0)^2}{4\tilde{\sigma}^2}}, \quad (190)$$

and d is chosen as in (189). In the absence of a gravitational time dilation the resulting frequency distribution \tilde{f} then reads, up to normalisation,

$$\begin{aligned} \tilde{f}(\omega) \\ \sim e^{-\frac{(\omega-\omega_0)^2}{2\tilde{\sigma}^2}} \cos^2 \left(\frac{\omega}{\omega_0} \left(\pi \left(n + \frac{1}{2}\right) - \frac{\varphi}{2} \right) + \frac{\varphi}{2} \right), \end{aligned} \quad (191)$$

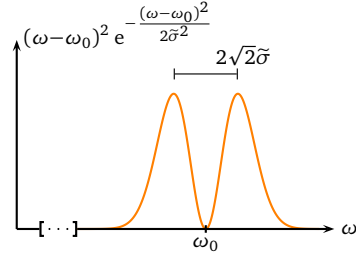
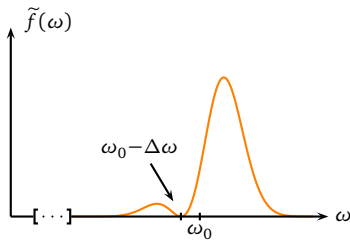


Figure 18: Sketch of leading term of the frequency distribution $\tilde{f}(\omega)$.

$n \in \mathbb{N}$. Since for $\omega_0 \gg \tilde{\sigma}$ the \cos^2 -part varies considerably slower than the exponential part one can expand the cosine about $\omega = \omega_0$:

$$\tilde{f}(\omega) \sim \frac{(\omega - \omega_0)^2}{\omega_0^2} e^{-\frac{(\omega-\omega_0)^2}{2\tilde{\sigma}^2}} + e^{-\frac{(\omega-\omega_0)^2}{2\tilde{\sigma}^2}} \cdot \mathcal{O} \left(\frac{(\omega-\omega_0)^4}{\omega_0^4} \right) \quad (192)$$

The leading term clearly represents the double-humped shape of \tilde{f} and the cut out frequency ω_0 , see Fig. 18. Via the first derivative one directly finds that the two humps are separated by $2\sqrt{2}\tilde{\sigma}$ to leading order.



But if the gravitational time dilation comes into play (e.g., by rotating the interferometer into the gravitational field) the zeros of the \cos^2 are slightly downshifted by $\Delta\omega$. Hence another frequency $\omega_0 - \Delta\omega$, in the neighbourhood of ω_0 , is cut out, see Fig. 19. From (188) it follows that $\Delta\omega$ is given by

$$\Delta\omega = \omega_0 \frac{\delta}{d + \delta}, \quad (193)$$

Figure 19: $\tilde{f}(\omega)$ for a nonvanishing gravitational time dilation. as long as $\omega_0 < 1/\delta$. In terms of ΔT and $\Delta\tau$ this reads:

$$\Delta\omega = \omega_0 \frac{\Delta\tau}{\Delta T + \Delta\tau} = \omega_0 \frac{\Delta\tau}{\Delta T} + \mathcal{O} \left(\frac{\Delta\tau^2}{\Delta T^2} \right). \quad (194)$$

Also the postselection probability needs to be considered. For the chosen preselection and postselection one obtains:

$$p = \frac{1 + \cos \varphi \operatorname{Re} \langle \psi_{+d+\delta}, \psi_{-d-\delta} \rangle}{2}. \quad (195)$$

If one restricts on wave packets with a simple phase $\psi(t) = |\psi(t)|e^{i\omega_0 t}$ the real part of the overlap can be written as

$$\begin{aligned} \operatorname{Re} \langle \psi_{+d+\delta}, \psi_{-d-\delta} \rangle &= \cos(2\omega_0 \delta + 2\omega_0 d) \int_{-\infty}^{\infty} |\psi(t+d+\delta)| |\psi(t-d-\delta)| dt \\ &\leq \cos(2\omega_0 \delta + 2\omega_0 d). \end{aligned} \quad (196)$$

Choosing d as given in (189) leads to

$$\operatorname{Re} \langle \psi_{+d+\delta}, \psi_{-d-\delta} \rangle \leq -\cos(\varphi - 2\omega_0 \delta) \approx -\cos \varphi. \quad (197)$$

Hence, to lowest order, one obtains

$$p \geq \frac{1 - \cos^2 \varphi}{2}. \quad (198)$$

Thus the optimal choice of $|\varphi|$ is a value around $\pi/2$ such that $p \geq \frac{1}{2}$.

Consider, e.g., photons with a mean frequency of $\omega_0 = 2 \cdot 10^{15}$ Hz and a controllable time delay of $\Delta T \equiv 2d = 2.35 \cdot 10^{-15}$ s (see eq. (189) for $n = 0$ and $\varphi = -\pi/2$) which corresponds to an additional path length of 706.37 nm. An interferometer with a surface of 2500 m^2 (which, in a quadratic case, corresponds to arm lengths of only 50 m) results in a gravitational time dilation of $\Delta\tau = 9.1 \cdot 10^{-22}$ s and in a downshift of $\Delta\omega = 0.77 \cdot 10^9$ Hz. Since it is no problem to create photons with a bandwidth of 10^9 Hz this downshift $\Delta\omega$ of the cut out frequency deforms the frequency distribution of the photons significantly.

This effect could be measured in the following way. Consider a glass tube which is filled with a gas whose atoms can be excited by photons with a frequency of ω_0 . If the photons have a frequency distribution like in Fig. 18, i.e. in the gravity free case, a certain number, which depends of the atom's line width, of photons are able to excite an atom of the gas. If, on the other hand, the gravitational time dilation downshifts the cut out frequency, like in Fig. 19, more photons will be absorbed by the gas, since one hump of the frequency distribution is shifted above the absorption frequency. So the rate of photons passing the glass tube could be decreased in a measurable way. A photon detector behind the glass tube could measure these changes of passing photons in dependence of the gravitational phase shift.

A concrete example could look as follows. Assume the glass tube is filled with a gas of ^{133}Cs atoms. Ignoring the hyperfine structure the transition of the D_2 line ($6^2S_{1/2} \rightarrow 6^2P_{3/2}$) of cesium can be exploited. The corresponding frequency of this transition [18] is given by $\omega_{\text{ex}} = 2.21 \cdot 10^{15}$ Hz. Conducting the experiment at room temperature, $T = 293$ K, the line width of the atoms is given by the Doppler width due to Doppler broadening. The Doppler

broadened line width is usually modelled by a Gaussian distribution [19] with a standard deviation of

$$\tilde{\sigma}_{\text{Dop}} = \sqrt{\frac{k_B T}{c^2 m_{\text{Cs}}}} \omega_{\text{ex}} . \quad (199)$$

Here k_B is the Boltzmann constant and m_{Cs} is the mass of a cesium atom. Since $m_{\text{Cs}} = 132.91 \text{ u} = 2.207 \cdot 10^{-25} \text{ kg}$ the line width of the transition has the standard deviation of $\tilde{\sigma}_{\text{Dop}} = 998.03 \cdot 10^6 \text{ Hz}$. If the pressure of the gas is sufficiently low pressure broadening can be neglected. In order to keep the calculations as simple as possible the 3-sigma rule⁹ is used here: Photons with a frequency outside of the interval $\Omega_{\text{ex}} \equiv [\omega_{\text{ex}} - 3\tilde{\sigma}_{\text{Dop}}, \omega_{\text{ex}} + 3\tilde{\sigma}_{\text{Dop}}]$ will not be absorbed by the cesium gas and therefore pass the glass tube. Hence, one can estimate that the rate η of photons passing the glass tube unhindered is at least

$$\eta \approx 1 - \int_{\Omega_{\text{ex}}} \tilde{f}(\omega) d\omega . \quad (200)$$

Figure 20 shows numerical results of the downshift of the cut out frequency due to the gravitational phase shift for the example of a cesium gas in the glass tube. The photon source was chosen to produce photons with a mean frequency of $\omega_0 = \omega_{\text{ex}}$, a bandwidth of $\tilde{\sigma} = 2 \cdot 10^9 \text{ Hz}$, and the controllable time delay is $\Delta T = 2d = 1.42 \cdot 10^{-15} \text{ s}$ (see eq. (189) for $n = 0$ and $\varphi = 0$).

Why does this method only probe the phase shift effect and not the gravitational time dilation? To see this one can assume that instead of causing a time dilation gravity would only cause an Aharonov-Bohm phase $\Phi = \omega_0 \Delta\tau$ between the two arms of the interferometer. The argument of the \cos^2 in the frequency distribution of the photon after the postselection (187) would then be given by $\omega d + \omega_0 \delta + \varphi/2$ instead of $\omega(d + \delta) + \varphi/2$. This can be seen by replacing $\delta \rightarrow 0$ and $\varphi \rightarrow \varphi + \Phi = \varphi + 2\omega_0 \delta$ in (184). Thus, in the Newtonian limit, the downshift of the cut out frequency would read

$$\Delta\omega^{\text{NL}} = \omega_0 \frac{\delta}{d} \quad \text{instead of} \quad \Delta\omega = \omega_0 \frac{\delta}{d + \delta} . \quad (201)$$

The difference between both is negligible small:

$$\Delta\omega^{\text{NL}} - \Delta\omega = \omega_0 \frac{\delta^2}{d^2} + \mathcal{O}\left(\frac{\delta^3}{d^3}\right) . \quad (202)$$

According to the lower right graph of Fig. 20 this difference would only be $3.5 \cdot 10^3 \text{ Hz}$. Thus there is no conceptual difference between the Newtonian limit and general relativistic time dilation since in both cases a downshift of the cut out frequency occurs, as well as the fact that the numerical difference has no measurable influence of the proposed experiment.

Note, that a major hindrance for this method is given by requirement that the precision of the additional controllable time delay ΔT needs to be of the order of the gravitational time

⁹The 3-sigma rule states that 99.7 % of the area of a Gaussian distribution is covered by plus/minus 3 standard deviations away from the mean.

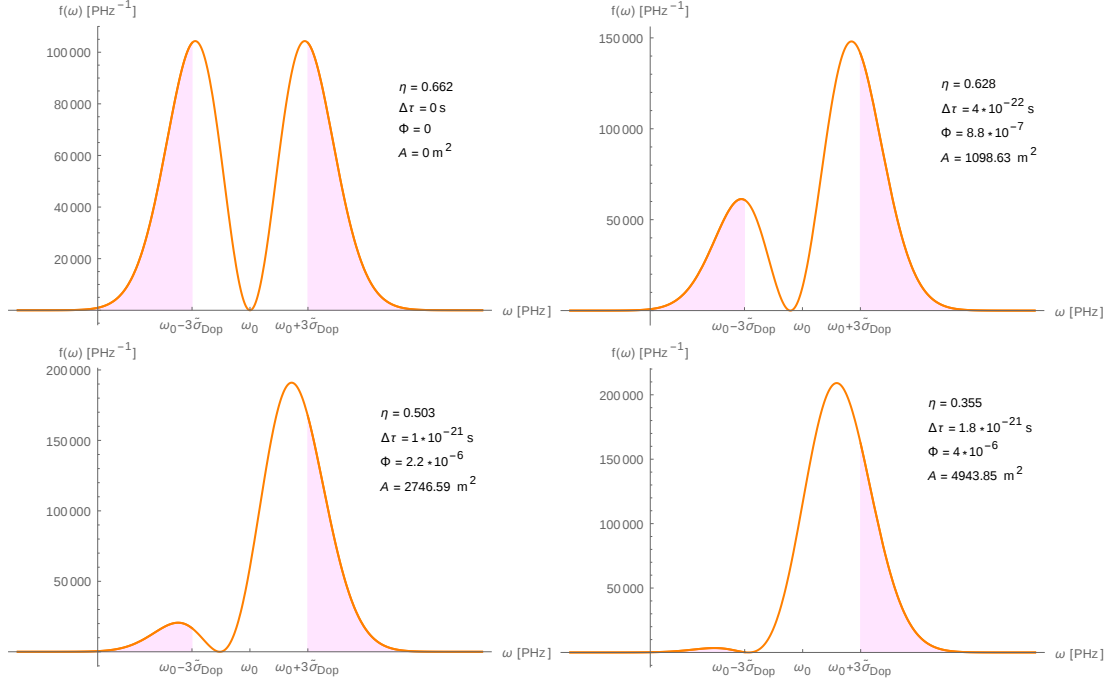


Figure 20: Plots of the frequency distribution \tilde{f} of the photon after the postselection. The parameters are chose as $\omega_0 = \omega_{\text{ex}} = 2.21 \cdot 10^{15}$ Hz, $\tilde{\sigma} = 2 \cdot 10^9$ Hz and $\Delta T = 2d = 1.42 \cdot 10^{-15}$ s. The pink area illustrates the frequency contribution of the photons which are outside of the interval $\Omega_{\text{ex}} \equiv [\omega_{\text{ex}} - 3\tilde{\sigma}_{\text{Dop}}, \omega_{\text{ex}} + 3\tilde{\sigma}_{\text{Dop}}]$ and therefore can not be absorbed by the cesium gas. Here σ_{Dop} represents the Doppler width of the cesium atoms (see eq. 199). One can see that already for a small gravitational phase shift of $\Phi = 4 \cdot 10^{-6}$ the rate of photons η at least passing the tube is decreased from 66.2% to 35.5%.

dilation $\Delta\tau$. Otherwise it is not possible to reach the double humped-shape of the frequency distribution \tilde{f} . Since with subnanopositioner elements one can control the additional time delay with a precision of $0.05 \text{ nm}/c = 0.17 \text{ as}$, the smallest possible interferometer for this method will have a surface of about $4.6 \cdot 10^5 \text{ m}^2$. This is four orders of magnitude smaller than 10^3 km^2 as suggested in [1].

6 Conclusion

In this thesis five methods to measure the effects of gravitational time dilation or gravitational phase shifts on single photons were presented. The improvement compared to the original publication [1] is summarised in the following.

In the first method the weak measurement formalism was applied in order to amplify the shifts in the mean frequency and in the mean arrival time of the photons due to the gravitational time dilation. The results show that considerably smaller interferometers can be used to measure the influence of gravitational time dilation on single photons compared to the ones discussed in [1]. Instead of interferometers with a surface of 10^3 km^2 (which is about the size of Cyprus) only 10^4 m^2 (which is about the size of a soccer field) could be enough to measure the gravitational time dilation. The improvement amounts to five orders of magnitude. The postselection probability was 10^{-8} in this example.

The second method was a technique to amplify a relative phase in an optical interferometer similar to the weak measurement formalism. The suggested set of parameters, given at the end of ch. 5.2, also assumed an interferometer with a surface of 10^4 m^2 . The resulting Aharonov-Bohm phase then is about $\Phi = 3.6 \cdot 10^{-6}$. Due to the amplification effect the effective relative phase was $\Phi/\varepsilon = 2 \cdot 10^{-2}$ since the chosen parameters lead to an amplification factor of $1/\varepsilon = 5.6 \cdot 10^3$ and a postselection probability of $3.2 \cdot 10^{-6}$. If, instead of photons, only classical light is of interest even smaller interferometers can be used since in such a case low postselection probabilities can be compensated by high laser intensities.

Introducing an additional controllable time delay on top of the gravitational time dilation was the main idea of the third method. This additional controllable time delay was chosen such that the sensitivity of the detection probabilities to the gravitational time dilation becomes maximal. Also here an improvement could be reached: The suggested parameters lead to an interferometer with a surface of 11.9 km^2 . This is an improvement of two orders of magnitude with respect to [1].

Method 4 exploited the occurrence of a double-humped shape of the photons if the time delay of the wave packets lies within a very narrow interval. To reach this narrow interval a controllable time delay on top of the gravitational time dilation was necessary. Inside this narrow interval the effect was not distinguishable from a phase shift effect. Currently available nanopositioner elements which have a resolution of 0.05 nm (which corresponds to a resolution of 0.17 as) would allow to use an interferometer with a surface of $2.7 \cdot 10^5 \text{ m}^2$. For optical photons the Aharonov-Bohm like phase shift would then be of the order of 10^{-4} . Since even smaller phase shifts can be measured with current technology, this method can not be viewed as an improvement but rather as a new method to detect phase shifts in quantum optical experiments.

The last method based on the idea that the gravitational phase shift causes a deformation of the frequency distribution of the postselected photons. These deformations could be measured in a spectroscopic experiment. Feasible experimental parameters lead to the possibility to measure a gravitational phase shift of about $\Phi = 3.3 \cdot 10^{-4}$ which corresponds to a surface of $4.6 \cdot 10^5 \text{ m}^2$. The postselection probability was larger than $1/2$. Also here, like in method 4, this can at least be seen as a new method to measure phase shifts.

Acknowledgements

I would like to thank Igor Pikovski and Magdalena Zych for fruitful discussions and encouragement during my studies. Many thanks to Časlav Brukner for the very interesting topic and his supervision of this thesis. Another thank you goes to Francesco Massa who kindly answered all my questions concerning the technical capabilities and feasibility of my ideas. I owe special thanks to my father who generously funded my studies and my life in Vienna. Also special thanks to my mother. Both taught me early on that education is very valuable and both having been very supportive during my university life. Last but not least I want to mention my girlfriend who shared her experiences with me and taught me how to stay the course. Thank you very much.

References

- [1] M. Zych, F. Costa, I. Pikovski, T. C. Ralph, and Č. Brukner. General relativistic effects in quantum interference of photons. *Class. Quantum Grav.*, 29:224010, October 2012.
- [2] M. Zych, F. Costa, I. Pikovski, and Č. Brukner. Quantum interferometric visibility as a witness of general relativistic proper time. *Nat. Commun.*, 2:505, October 2011.
- [3] J. C. Hafele and R. E. Keating. Around-the-World Atomic Clocks: Predicted Relativistic Time Gains. *Science*, 177:166–168, July 1972.
- [4] J. C. Hafele and R. E. Keating. Around-the-World Atomic Clocks: Observed Relativistic Time Gains. *Science*, 177:168–170, July 1972.
- [5] T. E. Cranshaw, J. P. Schiffer, and A. B. Whitehead. Measurement of the gravitational red shift using the mössbauer effect in Fe^{57} . *Phys. Rev. Lett.*, 4:163–164, Feb 1960.
- [6] R. V. Pound and G. A. Rebka. Apparent weight of photons. *Phys. Rev. Lett.*, 4:337–341, Apr 1960.
- [7] I. I. Shapiro, G. H. Pettengill, M. E. Ash, M. L. Stone, W. B. Smith, R. P. Ingalls, and R. A. Brockelman. Fourth test of general relativity: Preliminary results. *Phys. Rev. Lett.*, 20:1265, 1968.
- [8] B.-G. Englert. Fringe Visibility and Which-Way Information: An Inequality. *Phys. Rev. Lett.*, 77:2154–7, 1996.
- [9] D. M. Greenberger and A. Yasin. Simultaneous wave and particle knowledge in a neutron interferometer. *Physics Letters A*, 128(8):391 – 394, 1988.
- [10] J. v. Neumann. *Mathematical Foundations of Quantum Mechanics*. 1932.
- [11] Y. Aharonov, D. Z. Albert, and L. Vaidman. How the result of a measurement of a component of the spin of a spin- $\frac{1}{2}$ particle can turn out to be 100. *Phys. Rev. Lett.*, 60:1351–1354, Apr 1988.
- [12] I. M. Duck, P. M. Stevenson, and E. C. G. Sudarshan. The sense in which a ”weak measurement” of a spin- $\frac{1}{2}$ particle’s spin component yields a value 100. *Phys. Rev. D*, 40:2112–2117, Sep 1989.
- [13] R. Jozsa. Complex weak values in quantum measurement. *Phys. Rev. A*, 76:044103, Oct 2007.
- [14] H. F. Hofmann. Uncertainty limits for quantum metrology obtained from the statistics of weak measurements. *Phys. Rev. A*, 83:022106, Feb 2011.
- [15] J. C. Diels and W. Rudolph. *Ultrashort Laser Pulse Phenomena*. New York, Academic, 2006.

- [16] N. Brunner and C. Simon. Measuring small longitudinal phase shifts: Weak measurements or standard interferometry? *Phys. Rev. Lett.*, 105:010405, Jul 2010.
- [17] G. N. Gol'tsman, A. Korneev, I. Rubtsova, I. Milostnaya, G. Chulkova, O. Minaeva, K. Smirnov, B. Voronov, W. Słysz, A. Pearlman, A. Verevkin, and R. Sobolewski. Ultra-fast superconducting single-photon detectors for near-infrared-wavelength quantum communications. *Phys. stat. sol.*, 2:1480–1488, Mar 2005.
- [18] Th. Udem, J. Reichert, T. W. Hänsch, and M. Kourogi. Absolute optical frequency measurement of the cesium D_2 line. *Phys. Rev. A*, 62:031801, Aug 2000.
- [19] W. Demtröder. *Laser Spectroscopy 1*. Springer, 5th edition, 2014.

Tobias Schäfer

Curriculum vitae

Boltzmanngasse 5

Room: 3416

1090 Vienna

☎ +43 (1) 4277 72580

✉ tobias.schaefer@univie.ac.at

Education

- 2012–today **Master of Science**, *University of Vienna*, Austria.
2008–2012 **Bachelor of Science**, *Goethe Universität*, Frankfurt am Main, Germany, Minor in Economics.
2007–2008 **Civilian service**, *Refugee home for children and youth*, Germany.
2007 **Abitur**, *Heinrich-von-Kleist-Schule*, Eschborn, Germany.

Master's Thesis

- Title *Feasibility study for measurement of general relativistic time dilations and gravitational phase shifts on single photons*
Supervisor Univ.-Prof. Dr. Caslav Brukner

Bachelor's Thesis

- Title *Deviation from the exponential decay law in quantum mechanics*
Supervisors Prof. Dr. Dirk H. Rischke, Priv. Doz. Dr. Francesco Giacosa
Grade 1.0

Jobs, Teaching and Conferences

- 2014 Participant of the science conference *Quantum [Un]Speakables II: 50 Years of Bell's Theorem*, Vienna.
2010–2012 Editing lecture notes in *Statistical Physics* for publication by the Springer Verlag.
2011–2012 Tutor position in *Special Relativity and Quantum Mechanics*
2011 Tutor position in *Classical Mechanics*
2010–2011 Tutor position in *Electrodynamics*
2010 Tutor position in *Classical Mechanics*
2006 Summer job in the software company *Swissrisk Financial Systems* in Frankfurt am Main.